Stability Analysis and Control of Nonlinear, Symmetrically Coupled Systems, with Applications to Paralleled Power Converters

by

Ankur Garg

B.S., Case Western Reserve University (1996)

Submitted to the Department of Electrical Engineering and Computer Science
in partial fulfillment of the requirements for the degree of

Master of Science in Electrical Engineering and Computer Science

at the

MASSACHUSETTS INSTITUTE OF TECHNOLOGY

May 1998

Author_____
Department of Electrical Engineering and Computer Science
May 22, 1998

Certified by_____
George C. Verghese
Professor of Electrical Engineering
Thesis Supervisor

Certified by_____
David J. Perreault
Postdoctoral Associate in Electrical Engineering
Thesis Co-Supervisor

Accepted by_____
Arthur C. Smith
Chairman, Departmental Committee on Graduate Students

Stability Analysis and Control of Nonlinear, Symmetrically Coupled Systems, with Applications to Paralleled Power Converters

by
Ankur Garg

Submitted to the Department of Electrical Engineering and Computer Science
on May 8, 1998 in partial fulfillment of
the requirements for the degree of
Master of Science in Electrical Engineering

Abstract

Symmetric systems comprise identical subsystems coupled identically to each other. In most applications, these open-loop symmetrically-coupled subsystems have common feeds into other systems and feedback from other systems. Subsystems are often coupled symmetrically to achieve a large system rating as well as to improve reliability of the overall system through redundancy. Even if the individual subsystems are stable, when they are interconnected via linear or nonlinear mutual coupling, the overall system may not be stable. If the coupling is nonlinear, it becomes extremely difficult to set criteria that ensure the overall stability of the system, particularly if the nonlinearities involve non-differentiable functions such as max(.,.). Furthermore, such systems are also difficult to analyze due to their high order.

This thesis explores two avenues to assess the stability of open- and closed-loop symmetrically-coupled nonlinear systems. The first involves reducing the stability analysis of the overall symmetric nonlinear system to that of lower-order linear and nonlinear systems. The stability of these reduced-order subsystems can then be used to guarantee stability of the overall system. The second involves partitioning the state-space of a nonlinear system with piecewise affine dynamics into a number of closed cells, and then searching for a piecewise continuous Lyapunov function for the system.

The major physical model analyzed in this thesis is that of paralleled current-mode-controlled power converters with nonlinear couplings for realizing current sharing control. We will primarily consider current sharing schemes that employ the maximum of the individual cell currents as the coupling function.

Thesis Supervisor: George C. Verghese
Title: Professor of Electrical Engineering

Thesis Co-Supervisor: David J. Perreault
Title: Postdoctoral Associate in Electrical Engineering

Dedication

---

to

My Family...

My Parents,

and My Brother.

Acknowledgments

First and foremost, I must thank my incredible advisor, George Verghese. I don't know where I would be without his ideas, advice and guidance. Anytime I walked into his office discouraged and feeling as if I had run into a brick wall, he patiently led me through the problems and offered invaluable suggestions. And of course, despite his hectic schedule, he always had a few minutes to spare!

Second, I would like to thank Dave Perreault. His insights and constant assistance were invaluable to this thesis. He was always there when I had a question or two... well, ok ... usually it was more than just two! His door was always open to me and his enthusiasm was always encouraging. His wonderful sense of organization have made this thesis flow as beautifully as it does!

For helping me stay afloat and sane, thanks goes out to all the people in LEES and 10-082. Vivian was always there to help me through the tough days, and constantly offered to do all the administrative tasks that I wasn't even aware existed! Isaac and I crunched through unending problem sets together, talked and talked about everything and, of course, went out and painted the town red together. I think some people thought we were glued to each other... Vahe and James were always willing to help out when I was stuck - which was pretty often! Thanks guys for putting up with my constant questions and confusions. As for Jama, Chalee and Khurram, thanks for all the help and encouragement! And many thanks to Babak for helping me find George in the first place!

I must also thank all my close friends who allowed me to vent my frustrations over hours and hours of phone calls and were always there to help me through my periods of discouragement.

This thesis is dedicated to my family; my parents and my brother. Their patience in listening to me ramble on about my days at MIT still amazes me. I am forever grateful to them for all the advice and support they have given me over the years.

Contents

List of Figures

List of Tables

1 Introduction

Symmetric systems comprise identical subsystems coupled identically to each other. In most applications, these open-loop symmetrically-coupled subsystems have common feeds into other systems and common feedback from other systems. Subsystems are often coupled symmetrically to reduce the stress on individual subsystems as well as to improve reliability of the overall system through redundancy. Even if the individual subsystems are stable, when they are interconnected via linear or nonlinear mutual coupling, the overall system may not be stable. If the coupling is nonlinear, it becomes extremely difficult to set criteria that ensure the overall stability of the system, particularly if the nonlinearities involve non-differentiable functions such as max(.,.).

Analysis and control of large-scale symmetric systems with feedback is challenging due to both the size and the nature of the coupling present between subsystems. Some research into stability analysis for such symmetric systems has been directed toward systems with linear mutual coupling [1,12-15]. For nonlinear mutual couplings, the system may sometimes be linearized about a fixed operating point to perform a small-signal analysis in order to gauge stability [5,7]. Often, though, this is not possible if the coupling function is not differentiable, as is true in the case where the *maximum* of individual subsystem variables is used as the coupling function, for example. Piecewise or hybrid coupling feedback, as with the 'max' coupling, also often leads to a system that cannot be analyzed by linearization.

1.1 Overview

In this thesis, we will explore two main avenues to assess the stability of open- and closed-loop symmetrically-coupled nonlinear systems. For a system with a large number of coupled subsystems, it is first desirable to reduce the order of the system to make analysis and control tractable. A finite-order open-loop symmetrically-coupled system can be described by the state-space model

$$\begin{bmatrix} \dot{x}_1 \\ \dot{x}_2 \\ \vdots \\ \dot{x}_N \end{bmatrix} = \begin{bmatrix} A_1 & A_2 & \cdots & A_2 \\ A_2 & A_1 & \cdots & A_2 \\ \vdots & \vdots & & \vdots \\ A_2 & A_2 & \cdots & A_1 \end{bmatrix} \begin{bmatrix} x_1 \\ x_2 \\ \vdots \\ x_N \end{bmatrix} + \text{diag}(B)u, \tag{1.1a}$$

$$y = \text{diag}(C)x \tag{1.1b}$$

where x_i represents the state variables for the i^{th} subsystem, and there are N symmetrically-coupled subsystems. Lunze uses linear transformations to reduce the stability analysis of a linear symmetric system consisting of N subsystems to that of a model of order twice that of the subsystem order [1]. Model-order reduction techniques have been developed in the context of specific applications as well [12].

Although Lunze's analysis addresses only open-loop symmetrically-coupled systems, many cases of interest comprise symmetrically-coupled systems with common connections to other systems. Assuming that these feedback systems are represented by state variable vector w, the state equation in (1.1) now modifies to

$$\left[\begin{array}{c} \dot{x}_1 \\ \dot{x}_2 \\ \vdots \\ \dot{x}_N \\ \hline \dot{w} \end{array}\right] = \left[\begin{array}{cccc|c} A_1 & A_2 & \cdots & A_2 & BG \\ A_2 & A_1 & \cdots & A_2 & BG \\ \vdots & \vdots & & \vdots & \vdots \\ A_2 & A_2 & \cdots & A_1 & BG \\ \hline HC & HC & \cdots & HC & J \end{array}\right] \left[\begin{array}{c} x_1 \\ x_2 \\ \vdots \\ x_N \\ \hline w \end{array}\right]. \tag{1.2}$$

This thesis will show that model-order reductions, using techniques based upon those used by Lunze, are also possible for such closed-loop symmetric systems. We will extend our analysis further to include certain nonlinear couplings; specifically, it will be shown that it is possible to reduce the stability analysis of a class of symmetric nonlinear systems to that of lower-order linear and nonlinear systems; the stability of these reduced-order subsystems can be used to guarantee stability of the overall system.

The second avenue for stability assessment of symmetric systems, proposed by Johansson and Rantzer [2] for more general (hybrid) systems, involves partitioning the state-space of a nonlinear system with piecewise affine dynamics into a number of closed cells, and then searching for a piecewise continuous Lyapunov function to guarantee the stability of the overall system. Systems amenable to the treatment in [2] exist naturally as hybrid control systems and as approximations to other nonlinear systems, to cite only two examples.

The main physical model analyzed as an example throughout this thesis is that of paralleled current-mode-controlled power converters. In such a system, the paralleled power converter cells represent the symmetrically-coupled subsystems, and the load represents the feedback system. When paralleling converters, an additional control system is often implemented to ensure that the individual converters share the load current equally. The control system used for demonstration purposes in this thesis is based on each converter comparing its own current to the maximum of all currents. Such approaches are very popular in industry today, due to their ease of implementation and the availability of monolithic control circuits for this purpose [6]. Note that this 'max' current sharing scheme is merely one example of the possible nonlinear couplings that can be analyzed using the methods proposed in this thesis.

1.2 Thesis Contributions and Organization

As mentioned earlier, this thesis will explore several avenues to assess the stability of a symmetrically-coupled nonlinear system. In Chapter 2, we lay the groundwork for a system consisting of parallel current-mode-controlled converters with a 'max' current sharing scheme. This system provides the physical model that is analyzed throughout the thesis.

Chapters 3 and 4 show that the similarity transformation proposed in [1] to reduce the order of linearly coupled open-loop symmetric composite systems can be extended to symmetric systems with feedback and with nonlinear couplings. The similarity transformation will be applied to our nonlinear 'max' system to reduce the order of the system as well as assess its stability.

Chapter 5 will first cover the theory behind the method used by Johansson and Rantzer to find piecewise Lyapunov functions for hybrid systems [2]. We then attempt to find a piecewise quadratic Lyapunov function for the paralleled current-mode-controlled power converter example introduced in earlier chapters. Some limitations of the techniques developed by Johansson and Rantzer are exposed in this process.

2 *Paralleled Power Converters*

The physical model analyzed as an example throughout this thesis is that of paralleled power converters. Power converters are often paralleled to achieve a large system rating, to reduce the converter stresses, and to improve overall system reliability through redundancy. When paralleling converters, an additional control system is often implemented to ensure that the individual converters share the load current equally while maintaining stability and good regulation of the output voltage. Thus, it is important to be able to accurately predict the dynamics of a paralleled power converter system, including output voltage and load sharing control.

2.1 General Converter Model

Consider the averaged model for a current-mode-controlled power converter (Figure 2.1). The output voltage v_{out} of the converter is compared to a reference voltage v_{ref}, and the error between the two is used by the voltage control compensator to generate a reference current i_{ref} for the converter. Based upon this current reference, the current-mode-controlled power stage generates an average output current i_{out} into the load/filter combination.

If a voltage control loop compensator $G_c(s)$ of the form

$$G_c(s) = \frac{\kappa_c}{\tau_c s + 1} \tag{2.1}$$

is used, and we assume that the power stage gain may be well approximated as $H(s) \approx 1$, then we can form a circuit representation of the averaged model as shown in Figure 2.2, where $L = \tau_c / \kappa_c$ and $R = 1/\kappa_c$. This makes physical sense since the series combination of R and L represents the output impedance of the converter, and the output current i_{out} of the converter is delivered to the load/filter combination represented by the parallel combination of R_o and C_o. In an averaged

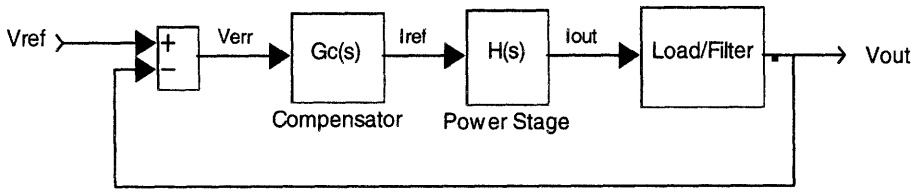

Figure 2.1: Averaged converter model.

sense, the converter appears as a voltage source with an output impedance. The output voltage regulation of the converter and its control bandwidth are dependent on the output impedance of the converter, and, in turn, on the compensator parameters κ_c and τ_c. In the general case, the actual form of the output impedance is determined by the feedback compensator $G_c(s)$ in the converter and the power-stage dynamics. Simple circuit analysis reveals the stability of this single converter.

2.2 Dual Converter Model

Suppose now that instead of just one current-mode-controlled converter supplying the parallel R_o, C_o load/filter combination, there are two, as shown in the averaged-model circuit representation of Figure 2.3.

As is obvious from this figure, if the real parts of the cell output impedances are zero, the paralleled converter system is unstable when the reference voltages are not equal. Even in the presence of output resistance, however, this system will not share current equally if the reference voltages are different. Furthermore, because the desire for good output voltage regulation generally causes the converter output resistances to be kept small, even small differences in the reference voltages will create large current imbalances.

These problems create the need for a current sharing control loop that modifies the reference voltages to attain equal current sharing and stability in this paralleled system. One popular way to implement such a control loop is the average current method, in which each power converter

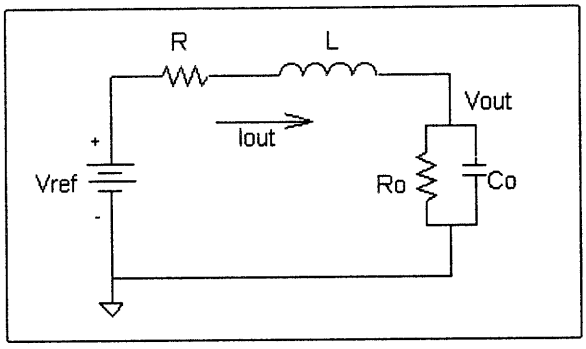

Figure 2.2: Averaged circuit model of a current-mode-controlled converter.

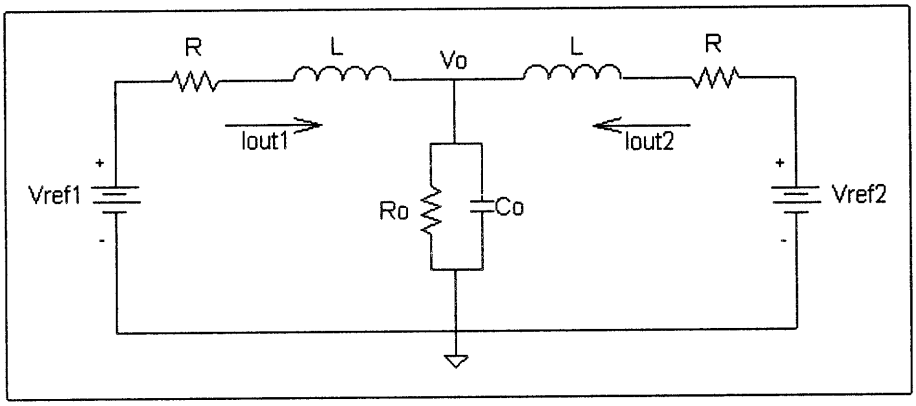

Figure 2.3: Initial averaged circuit model of a dual-cell converter system.

has a compensator that senses any imbalance between the average converter current and its own output current. When such an imbalance is detected, this compensator adjusts the local voltage reference until load sharing is achieved. The average current signal is generated on a common "share bus" by having each converter drive the bus through a resistor with a voltage proportional to its own output current.

Another possible method involves using the maximum converter current as a basis for implementing current sharing. In this case, each paralleled power converter has a compensator that senses any imbalance between the *maximum* converter current and its own output current. Again, when an imbalance is detected, the compensator adjusts the reference of the voltage amplifier until load sharing is achieved. The maximum current signal is also generated on a common "share bus", but this time each converter drives the bus, with a voltage proportional to its own output current, through a diode, instead of a resistor.

Thus, the control system used to achieve current sharing and stability can be linear or nonlinear in nature. As discussed in [12-15], some linear feedback control methods involve the feedback of the average current output of all the cells, as discussed earlier, or the current of a predetermined "master" cell. Although these are important control methods, many others exist that are based upon the feedback of quantities with inherently nonlinear dynamics, as introduced in [6-11]. These nonlinearities make it extremely difficult to set criteria that ensure the overall stability of the system, particularly if they involve non-differentiable functions such as max(.,.). It is precisely this nonlinear coupling that is analyzed as an example in this thesis.

2.2.1 'Max' Current Sharing Scheme

The averaged model for the dual-cell converter system under consideration is given in Figure 2.4. In this model,

$$v_{refi} = V_{basei} + \Delta v_{refi}, \tag{2.2}$$

i.e., we include the reference adjustments Δv_{refi} along with constant nominal base reference voltages V_{basei}. These non-identical base reference values allow us to account for the reality that no two converters will be absolutely identical.

To achieve current sharing, we can adjust the reference voltages via the state equations

$$\frac{d\Delta v_{ref1}}{dt} = k_1\left[i_{\max} - i_{out1}\right] - k_2\Delta v_{ref1} \tag{2.3a}$$

$$\frac{d\Delta v_{ref2}}{dt} = k_1\left[i_{\max} - i_{out2}\right] - k_2\Delta v_{ref2} \tag{2.3b}$$

in which k_1 and k_2 are strictly greater than zero. The k_1 terms adjust the references for current sharing while the k_2 decay terms keep the reference voltages from wandering away from their base values.

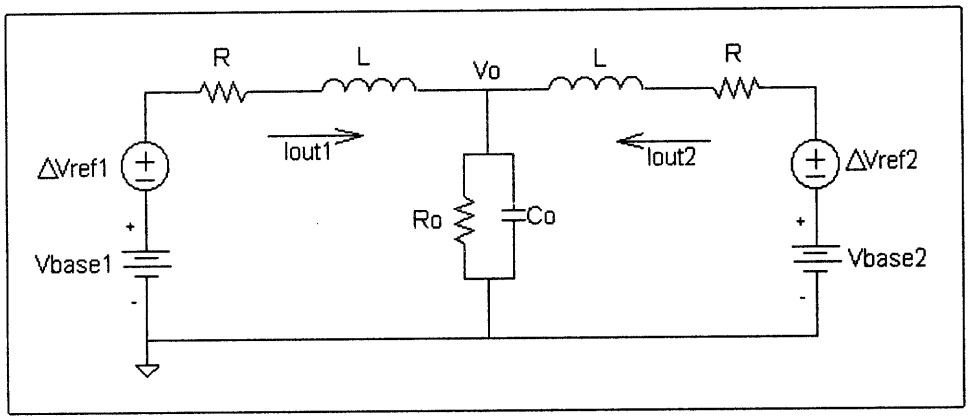

Figure 2.4: Averaged circuit model of a dual-cell converter system.

Based on the circuit model of Figure 2.4, the state equations for the converter output currents are given by

$$\frac{di_{outi}}{dt} = \frac{\Delta v_{refi} + V_{basei} - v_o - i_{outi}R}{L} \tag{2.4}$$

for $i = 1,2$, and the evolution of the output voltage is governed by

$$\frac{dv_o}{dt} = \frac{i_{out1} + i_{out2} - (v_o/R_o)}{C_o}. \tag{2.5}$$

Note that the state equations and circuit models presented in this section for a dual-cell paralleled power converter system can be easily extended to suit a system with N cells in parallel.

2.2.2 *'Max' Current Sharing Scheme using Unitrode's UC3907 IC*

A similar 'max' current sharing control scheme is implemented in Unitrode's *UC3907* current sharing IC. The averaged circuit model for this configuration is identical to that presented previously in Figure 2.4, where once again

$$v_{refi} = V_{basei} + \Delta v_{refi}, \tag{2.6}$$

where $\Delta v_{refi} \geq 0$, $i = 1,2$, and the constants V_{base1} and V_{base2} are the base values of v_{ref1} and v_{ref2} respectively.

The only difference between the two 'max' current sharing schemes is in the state equations for the reference adjustment. In this version, instead of decay terms, there are hard limits on the reference adjustment ranges, i.e. Δv_{refi} is now variable only within a saturation limit V_{sati}. Also, offset currents ΔI are used to drive the reference voltages towards their base value. The state equations for Δv_{ref1} and Δv_{ref2}, with k_1 strictly greater than zero, are

$$\frac{d\Delta v_{refi}}{dt} = k_1 \underbrace{\left[i_{\max} - i_{outi} - \Delta I \right]}_{\alpha_i} \tag{2.7}$$

for $i = 1,2$. Both these equations hold true only within the base and saturation bounds. Thus, the equations for the reference voltages can also be expressed as

$$\frac{d\Delta v_{refi}}{dt} = \begin{cases} k_1\alpha_i, & \text{for } \Delta v_{refi} \leq 0 \\ k_1\alpha_i, & \text{for } 0 \leq \Delta v_{refi} \leq V_{sati} \\ 0, & \text{for } \Delta v_{refi} \geq V_{sati} \end{cases} \qquad \text{for } \alpha_i > 0 \tag{2.8a}$$

$$\frac{d\Delta v_{refi}}{dt} = \begin{cases} 0, & \text{for } \Delta v_{refi} \leq 0 \\ k_1\alpha_i, & \text{for } 0 \leq \Delta v_{refi} \leq V_{sati} \\ k_1\alpha_i, & \text{for } \Delta v_{refi} \geq V_{sati} \end{cases} \qquad \text{for } \alpha_i < 0 \tag{2.8b}$$

The block diagram for this system is shown in Figure 2.5. The saturating integrators have a lower saturation limit of zero. The configuration used for the current sharing scheme is identical to that used by Unitrode's *UC3907* Load Share Controller IC.

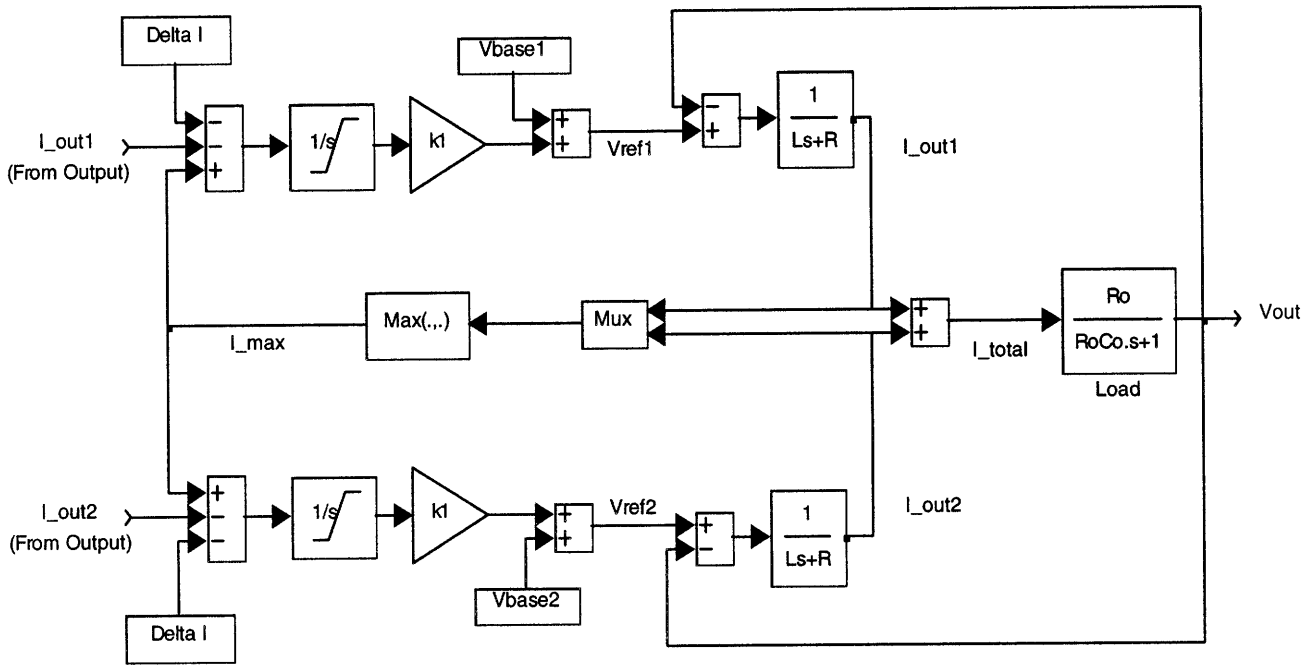

Figure 2.5: Nonlinear dual-cell converter system.

The ΔI term in (2.7) is introduced due to practical considerations. Without the ΔI term, there is no signal driving the reference voltage adjustment of the highest current cell. Noise terms can therefore cause this reference voltage to drift to its maximum value. Because the adjustment ranges of the reference voltages are not identical, cells with a lower maximum adjustment value will not be able to adjust their references to achieve current sharing. The ΔI term forces the highest current cell reference voltage towards its base value. This guarantees that the cell with the highest base reference will soon become the master, and that the other cells will be able to adjust themselves to achieve current sharing. Since all cells will adjust their currents to be ΔI below that of the master, the ΔI term also serves the secondary function of keeping the master status from chattering among cells in steady state. It follows then that ΔI must be small compared to i_{outi}, but large compared to the noise at the input of the reference adjustment

amplifiers of the individual cells. Note that the functionality of the ΔI term is similar to that of the proportional decay term introduced in the previous section.

With the current-sharing control in place, the state equations for the output currents and the output voltage are still given by (2.4) and (2.5) respectively.

2.2.3 Simplified Model without Load Dynamics

In order to simplify the analysis, the setup that will be studied in parts of later chapters is that of the dual-cell converter system without load dynamics. As shown in Figure 2.6, the load in this case can be modeled as a constant current source I_{out}. For convenience, we let $I_{out} = 0$, i.e. $i_{out2} = -i_{out1}$. In this case, the converter with the maximum current is the one carrying a positive output current. Note that a constant output current of zero does not affect the transient response of this system. If this current was some nonzero constant value, it would merely introduce an offset into the analysis.

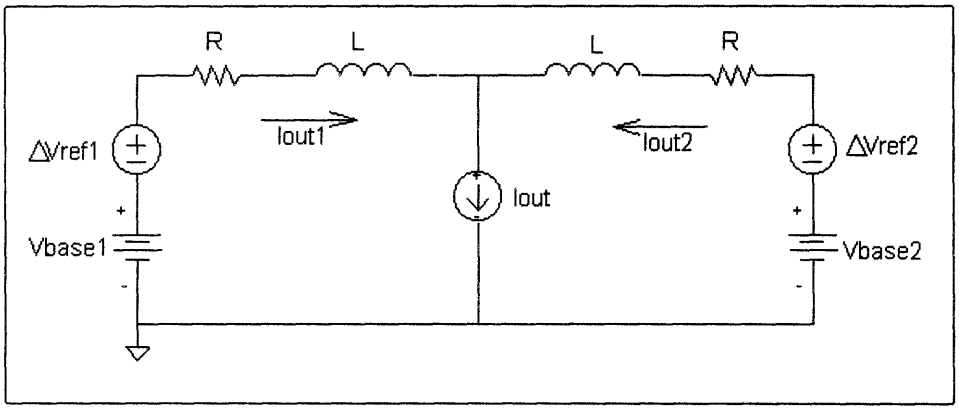

Figure 2.6: Load modeled as a constant current source.

3 *Symmetric Systems with Nonlinear Couplings*

For a system with a large number of coupled subsystems, it is desirable to reduce the order of the system. Lunze uses linear transformations to reduce the stability analysis of a linear symmetric system consisting of N subsystems to that of a model of order twice that of the subsystem order [1]. Lunze's analysis addresses only open-loop symmetrically-coupled systems, and not the closed-loop case. A simple example of a closed-loop symmetric system involves a paralleled dual-cell power converter with a load. In such a case the two power converter cells represent the two symmetrically-coupled subsystems and the load represents the feedback system. In this chapter, we will first extend Lunze's analysis to incorporate symmetric systems with common feedback through other systems, and then extend the analysis even further to include nonlinear coupling functions. It will be shown that it is often possible to reduce the stability analysis of a symmetric system with nonlinear couplings to that of lower-order linear and nonlinear systems; the stability of these reduced-order subsystems can be used to guarantee stability of the overall system.

3.1 Lunze's Analysis

In Chapter 12 of his book [1], Lunze uses linear transformations to reduce the stability analysis of a linear symmetric system consisting of N identical subsystems to that of a model of order twice that of the subsystem order n. The N subsystems of the plant are each described by

$$\dot{x}_i = A_{Lo}x_i + Bu_i + Es_i, \quad x_i(0) = x_{i0} \tag{3.1a}$$

$$y_i = Cx_i \tag{3.1b}$$

$$z_i = C_z x_i, \quad (i = 1,2,\ldots,N) \tag{3.1c}$$

with identical matrices for all subsystems. The interconnections are described by

$$s = Lz, \tag{3.2}$$

where the block 'symmetric' interconnection matrix L is given by

$$L = \begin{bmatrix} L_d & L_q & \cdots & L_q \\ L_q & L_d & \cdots & L_q \\ \vdots & \vdots & & \vdots \\ L_q & L_q & \cdots & L_d \end{bmatrix}, \tag{3.3}$$

and where s and z denote the vectors obtained by stacking the s_i and z_i respectively. These equations reflect the identical nature of the subsystems and the symmetric nature of their interconnections. The overall system description is given by

$$\dot{x} = \underbrace{\begin{bmatrix} A_{Lorig} + EL_dC_z & EL_qC_z & \cdots & EL_qC_z \\ EL_qC_z & A_{Lorig} + EL_dC_z & \cdots & EL_qC_z \\ \vdots & \vdots & & \vdots \\ EL_qC_z & EL_qC_z & \cdots & A_{Lorig} + EL_dC_z \end{bmatrix}}_{A_L} x + \mathrm{diag}(B)u \tag{3.4a}$$

$$y = \mathrm{diag}(C)x \tag{3.4b}$$

where $x = \begin{bmatrix} x_1^T & \cdots & x_N^T \end{bmatrix}^T$, and similarity for u and y. The length of x is Nn, where n is the order of each individual subsystem.

Using the linear transformation

$$\tilde{x} = T_L x \tag{3.5}$$

with

$$T_L = \frac{1}{N}\left[\begin{array}{cccc|c} (N-1)I & -I & \cdots & -I & -I \\ -I & (N-1)I & \cdots & -I & -I \\ \vdots & \vdots & & \vdots & \vdots \\ -I & -I & \cdots & (N-1)I & -I \\ \hline I & I & \cdots & I & I \end{array}\right] \tag{3.6a}$$

and its inverse

$$T_L^{-1} = \left[\begin{array}{cccc|c} I & 0 & \cdots & 0 & I \\ 0 & I & \cdots & 0 & I \\ \vdots & \vdots & & \vdots & \vdots \\ 0 & 0 & \cdots & I & I \\ \hline -I & -I & \cdots & -I & I \end{array}\right], \tag{3.6b}$$

the A_L matrix transforms to

$$\tilde{A}_L = T_L A_L T_L^{-1} = \left[\begin{array}{cccc|c} A_d & 0 & \cdots & 0 & 0 \\ 0 & A_d & \cdots & 0 & 0 \\ \vdots & \vdots & & \vdots & \vdots \\ 0 & 0 & \cdots & A_d & 0 \\ \hline 0 & 0 & & 0 & A_c \end{array}\right], \tag{3.7}$$

where

$$A_d = A_{Lo} + E\left(L_d - L_q\right)C_z, \tag{3.8a}$$

$$A_c = A_{Lo} + E\left[L_d + (N-1)L_q\right]C_z\,. \tag{3.8b}$$

Lunze thereby reduces the stability analysis of this nNth-order overall system to that of two nth-order matrices A_d and A_c. Note from (3.5) and (3.6) that $\tilde{x}_N$ is the *average* value of the original state variables x_i, and $\tilde{x}_i$ for $i = 1,2,..,(N-1)$ is the *deviation* of x_i from the average. Following the notation used by Thottuvelil and Verghese [12], we will refer to the $(N-1)$ subsystems

described by A_d as the *differential-mode* configurations, and the one subsystem described by A_c as the *common-mode* configuration. Thus, the stability of the overall system depends only upon the stability of one differential-mode and one common-mode system, each of order n [1]. In Appendix A, we show that it is possible to determine the form of the Lyapunov function for the original system, assuming ones exist for the reduced-order systems.

3.2 Symmetric Systems with Feedback

Lunze's analysis addresses only open-loop symmetrically-coupled systems, and not symmetrically-coupled systems with feedback. A simple example of a feedback case involves a paralleled dual-cell power converter system with a load. In such a case the two converter cells represent the two symmetrically-coupled subsystems, and the load represents the feedback system. Thottuvelil and Verghese [12] assess the small-signal stability of such paralleled converter systems feeding a common load.

Recall that there are N symmetrically-coupled subsystems, each of order n, and the interconnected system is governed by (3.4). We now introduce common feedback around the symmetric system, using an m^{th} order system with state vector w in the feedback path. The resulting closed-loop system is described as follows:

$$\begin{bmatrix} \dot{x} \\ \hline \dot{w} \end{bmatrix} = \underbrace{\left[\begin{array}{cccc|c} A_{Lo}+EL_dC_z & EL_qC_z & \cdots & EL_qC_z & BG \\ EL_qC_z & A_{Lo}+EL_dC_z & \cdots & EL_qC_z & BG \\ \vdots & \vdots & & \vdots & \vdots \\ EL_qC_z & EL_qC_z & \cdots & A_{Lo}+EL_dC_z & BG \\ \hline HC & HC & \cdots & HC & J \end{array}\right]}_{A} \begin{bmatrix} x \\ \hline w \end{bmatrix} \tag{3.9}$$

The matrix G describes the *identical* influence of the feedback system's state vector on each subsystem, whereas the matrix H describes the influence of the *sum* of subsystem outputs on the feedback system. The matrix J governs the evolution of the isolated system in the feedback path.

We now modify the similarity transformation T_L used by Lunze to accommodate the feedback system. The similarity transformation T_L is still necessary to transform the N state variables x_i

associated with the symmetrically-coupled subsystems. The state vector w associated with the feedback system should not be affected by this transformation, however. Thus, we want a new transformation matrix T such that

$$\left[\frac{\tilde{x}}{w}\right] = T\left[\frac{x}{w}\right] \tag{3.10}$$

Under these conditions, T must be defined as

$$T = \left[\begin{array}{c|c} T_L & 0 \\ \hline 0 & I \end{array}\right] \tag{3.11a}$$

where I is simply the identity matrix. Then,

$$T^{-1} = \left[\begin{array}{c|c} T_L^{-1} & 0 \\ \hline 0 & I \end{array}\right]. \tag{3.11b}$$

Through T, our overall system matrix A now transforms to

$$\tilde{A} = TAT^{-1} = \left[\begin{array}{cccc|cc} A_d & 0 & \cdots & 0 & 0 & 0 \\ 0 & A_d & \cdots & 0 & 0 & 0 \\ \vdots & \vdots & & \vdots & \vdots & \vdots \\ 0 & 0 & \cdots & A_d & 0 & 0 \\ \hline 0 & 0 & \cdots & 0 & A_c & BG \\ 0 & 0 & \cdots & 0 & NHC & J \end{array}\right] = \left[\begin{array}{c|c} \mathrm{diag}(A_d) & 0 \\ \hline 0 & A_{cc} \end{array}\right] \tag{3.12}$$

where again

$$A_d = A_{Lo} + E\left(L_d - L_q\right)C_z, \tag{3.13a}$$

$$A_c = A_{Lo} + E\left[L_d + (N-1)L_q\right]C_z \tag{3.13b}$$

and we define A_{cc} such that

$$A_{cc} = \begin{bmatrix} A_c & BG \\ NHC & J \end{bmatrix}. \tag{3.13c}$$

The upper diagonal block consisting of A_d matrices in (3.12) once again represents the differential-mode configurations for the transformed system. The lower diagonal block represented by A_{cc} is now the common-mode configuration for the closed-loop system. Note that only the common-mode part of the open-loop system engages the feedback system, because we are feeding back the sum of the individual outputs. The differential-modes turn out to be unobservable and uncontrollable. Once again we have reduced the stability analysis of the overall system to the stability analysis of one differential-mode and one common-mode system, except now the order of the common-mode circuit is not n, but $n+m$ instead.

Before we continue, note that the state variables associated with the $(N-1)$ differential-mode subsystems, each described by the matrix A_d, are $\tilde{x}_1$ through $\tilde{x}_{N-1}$. The state variables associated with the common-mode system, described by A_{cc}, are $\tilde{x}_N$ and w. In order to simplify future discussion, let us introduce the vector $\tilde{z}$ to represent all the state variables associated with the common-mode configuration, i.e. $\tilde{z} = \begin{bmatrix} \tilde{x}_N{}^T & w^T \end{bmatrix}^T$.

3.3 Nonlinear Couplings

It is possible to reduce the order of an open- or closed-loop symmetrically-coupled system with *nonlinear* couplings by taking advantage of its symmetry in a manner identical to the method outlined in the previous section to reduce the order of a linear symmetrically-coupled system. The stability of the overall nonlinear system can then be assessed through the stability of the reduced order linear and nonlinear systems.

Suppose we had a linear system described by

$$\dot{x} = Ax\,. \tag{3.14a}$$

If we wished to introduce nonlinearity into this system, we would simply introduce a nonlinear function $f(x)$ into our system description as shown below:

$$\dot{x} = Ax + f(x). \tag{3.14b}$$

Now that we have the general form of a nonlinear system, let us return to the symmetrically-coupled system with feedback as introduced in the previous section. We will start with a "pre-transformed" system and work backwards. Recall the transformed system

$$\begin{bmatrix} \dot{\tilde{x}}_1 \\ \dot{\tilde{x}}_2 \\ \vdots \\ \dot{\tilde{x}}_{N-1} \\ \hline \dot{\tilde{z}} \end{bmatrix} = \underbrace{\left[\begin{array}{cccc|c} A_d & 0 & \cdots & 0 & 0 \\ 0 & A_d & \cdots & 0 & 0 \\ \vdots & \vdots & & \vdots & \vdots \\ 0 & 0 & \cdots & A_d & 0 \\ \hline 0 & 0 & & 0 & A_{cc} \end{array}\right]}_{\tilde{A}} \begin{bmatrix} \tilde{x}_1 \\ \tilde{x}_2 \\ \vdots \\ \tilde{x}_{N-1} \\ \hline \tilde{z} \end{bmatrix}. \tag{3.15}$$

If the upper or lower triangle of this matrix $\tilde{A}$ had nonzero entries, its stability would still depend only upon the stability of matrices A_d and A_{cc}. Adding entries in either triangle would add linear couplings to our system. If we wish to add nonlinear couplings, we will have to add a vector of nonlinearities, as shown below:

$$\begin{bmatrix} \dot{\tilde{x}}_1 \\ \dot{\tilde{x}}_2 \\ \vdots \\ \dot{\tilde{x}}_{N-1} \\ \hline \dot{\tilde{z}} \end{bmatrix} = \underbrace{\left[\begin{array}{cccc|c} A_d & 0 & \cdots & 0 & 0 \\ 0 & A_d & \cdots & 0 & 0 \\ \vdots & \vdots & & \vdots & \vdots \\ 0 & 0 & \cdots & A_d & 0 \\ \hline 0 & 0 & & 0 & A_{cc} \end{array}\right]}_{\tilde{A}} \begin{bmatrix} \tilde{x}_1 \\ \tilde{x}_2 \\ \vdots \\ \tilde{x}_{N-1} \\ \hline \tilde{z} \end{bmatrix} + \begin{bmatrix} f_1 \\ f_2 \\ \vdots \\ f_{N-1} \\ f_N \end{bmatrix} \tag{3.16}$$

Note that f_1 through f_{N-1} are vectors of length n, while f_N is a vector of length $n+m$ described by $f_N = \begin{bmatrix} f_{N1}{}^T & f_{N2}{}^T \end{bmatrix}^T$.

It is now possible to gauge the stability of the system (3.16) based merely on two linear systems described by A_d and A_{cc}, as before, as long as the nonlinear coupling for each block is well-behaved and dependent only upon the parameters in the blocks preceding it, i.e.

$$\dot{\tilde{x}}_i = A_d\tilde{x}_i + f_i(\tilde{x}_1, \tilde{x}_2..., \tilde{x}_{i-1}), \tag{3.17a}$$

$$\dot{\tilde{z}} = A_{cc}\tilde{z} + f_N(\tilde{x}_1, \tilde{x}_2..., \tilde{x}_{N-1}) \tag{3.17b}$$

for $i = 1,2,..,(N-1)$. From (3.17a), the state-evolution equations for $\tilde{x}_1$ and $\tilde{x}_2$ with are

$$\dot{\tilde{x}}_1 = A_d\tilde{x}_1, \tag{3.18a}$$

$$\dot{\tilde{x}}_2 = A_d\tilde{x}_2 + f_2(\tilde{x}_1). \tag{3.18b}$$

If A_d is stable, we know that $\tilde{x}_1$ decays exponentially to zero. Now, assume that the nonlinear function $f_2(\tilde{x}_1)$ is Lipschitz about the origin, i.e.

$$|f_2(\tilde{x}_1)| \leq M|\tilde{x}_1|, \tag{3.19}$$

Because $\tilde{x}_1$ decays exponentially to zero, $M|\tilde{x}_1|$ also decays exponentially to zero. Consequently, from (3.19), $f_2(\tilde{x}_1)$ decays exponentially to zero. The solution to (3.18b) is given by

$$\tilde{x}_2 = e^{A_d t}\tilde{x}_2(0) + \int_0^t e^{A_d(t-\tau)} f_2(\tilde{x}_1(\tau))\, d\tau \tag{3.20}$$

Taking norms on both sides of (3.20) and using norm inequalities reveal that for an exponentially stable system A_d with an exponentially bounded input $f_2(\tilde{x}_1)$ as given in (3.18b), the state vector $\tilde{x}_2$ decays exponentially as well. This argument can be similarly extended to show that, in general, if the functions f_i are Lipschitz, they will tend to zero exponentially as the $\tilde{x}_j$ tend to zero exponentially, for $j = 1,2,..,(i-1)$, and thus for stable A_d and A_{cc}, the system (3.16) is stable.

Note that the coupling in (3.17) reduces in the linear case to a *lower* triangular perturbation of $\tilde{A}$ in (3.15). One could also consider a nonlinear coupling that reduces to an *upper* triangular perturbation of $\tilde{A}$ in the linear case. Taking these nonlinear couplings back through the similarity transformation will provide us with a special class of nonlinear systems that can be easily analyzed via the transformation.

For an N-cell symmetrically-coupled system with feedback, the introduction of nonlinear coupling terms is represented by

$$\begin{bmatrix} \dot{\tilde{x}}_1 \\ \dot{\tilde{x}}_2 \\ \vdots \\ \dot{\tilde{x}}_{N-1} \\ \hline \dot{\tilde{z}} \end{bmatrix} = \underbrace{\left[\begin{array}{cccc|c} A_d & 0 & \cdots & 0 & 0 \\ 0 & A_d & \cdots & 0 & 0 \\ \vdots & \vdots & & \vdots & \vdots \\ 0 & 0 & \cdots & A_d & 0 \\ \hline 0 & 0 & \cdots & 0 & A_{cc} \end{array}\right]}_{\tilde{A}} \begin{bmatrix} \tilde{x}_1 \\ \tilde{x}_2 \\ \vdots \\ \tilde{x}_{N-1} \\ \hline \tilde{z} \end{bmatrix} + \underbrace{\begin{bmatrix} 0 \\ f_2(\tilde{x}_1) \\ f_3(\tilde{x}_1, \tilde{x}_2) \\ \vdots \\ \hline f_N(\tilde{x}_1, \tilde{x}_2, .., \tilde{x}_{N-1}) \end{bmatrix}}_{\tilde{F}}. \tag{3.21}$$

Remembering that

$$\begin{bmatrix} \tilde{x}_1 \\ \vdots \\ \tilde{x}_{N-1} \\ \hline \tilde{z} \end{bmatrix} = T \begin{bmatrix} x_1 \\ \vdots \\ x_{N-1} \\ \hline z \end{bmatrix} \tag{3.22}$$

and $\tilde{A} = TAT^{-1}$, we can rewrite our transformed system as

$$T \begin{bmatrix} \dot{x}_1 \\ \vdots \\ \dot{x}_{N-1} \\ \hline \dot{z} \end{bmatrix} = \left(TAT^{-1}\right) T \begin{bmatrix} x_1 \\ \vdots \\ x_{N-1} \\ \hline z \end{bmatrix} + \tilde{F}, \tag{3.23}$$

Reversing the similarity transformation then results in

$$\begin{bmatrix} \dot{x}_1 \\ \vdots \\ \dot{x}_{N-1} \\ \hline \dot{z} \end{bmatrix} = A \begin{bmatrix} x_1 \\ \vdots \\ x_{N-1} \\ \hline z \end{bmatrix} + T^{-1}\tilde{F} \tag{3.24}$$

Thus, remembering that $z = \begin{bmatrix} x_N{}^T & w^T \end{bmatrix}^T$ and $f_N = \begin{bmatrix} f_{N1}{}^T & f_{N2}{}^T \end{bmatrix}^T$, the original system is now represented by

$$\begin{bmatrix} \dot{x}_1 \\ \dot{x}_2 \\ \dot{x}_3 \\ \vdots \\ \dot{x}_{N-1} \\ \hline \dot{x}_N \\ \dot{w} \end{bmatrix} = A \begin{bmatrix} x_1 \\ x_2 \\ x_3 \\ \vdots \\ x_{N-1} \\ \hline x_N \\ w \end{bmatrix} + \underbrace{\begin{bmatrix} f_{N1}(\tilde{x}_1, \tilde{x}_2, .., \tilde{x}_{N-1}) \\ f_{N1}(\tilde{x}_1, \tilde{x}_2, .., \tilde{x}_{N-1}) + f_2(\tilde{x}_1) \\ f_{N1}(\tilde{x}_1, \tilde{x}_2, .., \tilde{x}_{N-1}) + f_3(\tilde{x}_1, \tilde{x}_2) \\ \vdots \\ f_{N1}(\tilde{x}_1, \tilde{x}_2, .., \tilde{x}_{N-1}) + f_{N-1}(\tilde{x}_1, \tilde{x}_2, .., \tilde{x}_{N-2}) \\ \hline f_{N1}(\tilde{x}_1, \tilde{x}_2, .., \tilde{x}_{N-1}) - \sum_{i=1}^{N-1} f_i(\tilde{x}_1, \tilde{x}_2, .., \tilde{x}_{i-1}) \\ f_{N2}(\tilde{x}_1, \tilde{x}_2, .., \tilde{x}_{N-1}) \end{bmatrix}}_{F}, \tag{3.25}$$

where

$$\tilde{x}_i = x_i - \frac{1}{N}\sum_{j=1}^{N} x_j \tag{3.26}$$

for $i = 1,2,..,(N-1)$.

Thus, when the similarity transformation is reversed, the nonlinear couplings $f_i(\tilde{x}_1, \tilde{x}_2, .., \tilde{x}_{i-1})$ that were introduced into the reduced-order system become functions of very special linear combinations of all the original state variables of the symmetrically-coupled systems. Note that the nonlinear couplings are not functions of any of the state variables associated with the feedback systems.

3.4 A Special Class of Nonlinear Couplings

Let us examine a special class of nonlinear couplings which can be applied to a system in a manner consistent with the previous section. A general system without nonlinearities is represented by

$$\begin{bmatrix} \dot{x} \\ \dot{w} \end{bmatrix} = A \begin{bmatrix} x \\ w \end{bmatrix} \tag{3.27}$$

where $x = \begin{bmatrix} x_1^T & \cdots & x_N^T \end{bmatrix}^T$ represents the state variables for the symmetrically-coupled subsystems, each of order n, and w represents the state vector for the feedback system.

Now, let's add some nonlinear couplings to this simple system. Assume that all subsystems have identical nonlinear couplings $g(x)$ and there are no nonlinear couplings present in the feedback systems. Our system can now be modified to include $g(x)$, as shown below:

$$\begin{bmatrix} \dot{x}_1 \\ \vdots \\ \dot{x}_N \\ \hline \dot{w} \end{bmatrix} = A \begin{bmatrix} \dot{x}_1 \\ \vdots \\ \dot{x}_N \\ \hline \dot{w} \end{bmatrix} + \begin{bmatrix} g(x) \\ \vdots \\ g(x) \\ \hline 0 \end{bmatrix} \tag{3.28}$$

Applying the similarity transformation T defined in (3.11) to our system yields

$$\begin{bmatrix} \dot{\tilde{x}}_1 \\ \vdots \\ \dot{\tilde{x}}_{N-1} \\ \dot{\tilde{x}}_N \\ \hline \dot{w} \end{bmatrix} = TAT^{-1} \begin{bmatrix} \tilde{x}_1 \\ \vdots \\ \tilde{x}_{N-1} \\ \tilde{x}_N \\ \hline w \end{bmatrix} + T \begin{bmatrix} g(x) \\ \vdots \\ g(x) \\ g(x) \\ \hline 0 \end{bmatrix} = TAT^{-1} \begin{bmatrix} \tilde{x}_1 \\ \vdots \\ \tilde{x}_{N-1} \\ \tilde{x}_N \\ \hline w \end{bmatrix} + \begin{bmatrix} 0 \\ \vdots \\ 0 \\ g(x) \\ \hline 0 \end{bmatrix} \tag{3.29}$$

Recall that the structure of the transformed A matrix, or TAT^{-1}, is block diagonal, i.e.

$$\tilde{A} = TAT^{-1} = \begin{bmatrix} \text{diag}(A_d) & 0 \\ 0 & A_{cc} \end{bmatrix} \tag{3.30}$$

Here, the differential-mode is represented by the block diagonal matrix diag(A_d) and corresponding state variables $\tilde{x}_1$ through $\tilde{x}_{N-1}$; the common-mode is represented by matrix A_{cc} and corresponding state variables $\tilde{x}_N$ and w. As expected, the transformation T isolates the nonlinearity $g(x)$ of the original system into the common-mode subsystem. The differential-mode subsystems are now linear, and their stability can be assessed from the stability of A_d. Thus, we have isolated the nonlinearity to a single subsystem with the transformation T, thereby significantly simplifying our original problem.

Note that if $g(x)$ is only a function of the state variables $\tilde{x}_1$ through $\tilde{x}_{N-1}$, and it exponentially decays to zero as these state variables exponentially decay to zero, the stability of the common-mode configuration can be assessed simply from the stability of A_{cc}. As discussed in the previous section, it is guaranteed that $g(\tilde{x}_1, \tilde{x}_2, .., \tilde{x}_{N-1})$ will decay to zero as x_1 through x_{N-1} decay to zero if $g(\tilde{x}_1, \tilde{x}_2, .., \tilde{x}_{N-1})$ is Lipschitz at the origin.

These cases represent one of the many classes of nonlinear couplings which can be handled by the analysis performed in this chapter. Note that our transformation T will remain valid even if $g(x)$ does not adhere to the above mentioned constraints. Similarly, along with symmetrical nonlinear couplings $g(x)$ in the subsystems, we could also introduce nonzero nonlinear couplings in the feedback systems. These would simply introduce nonlinearities in the common-mode configuration of the transformed system. The differential-mode system would still remain linear.

3.5 Further Extensions

Let us now briefly examine the case where nonlinear couplings are introduced in both the symmetrically-coupled subsystems as well as the feedback systems. Now, we lift all constraints initially placed upon these couplings. Recall that $x = \begin{bmatrix} x_1^T & \cdots & x_N^T \end{bmatrix}^T$ represents the state

variables for the symmetrically-coupled subsystems, each of order n, and w represents the state vector for the feedback system.

As an example, we will examine the simple setup shown in Figure 3.1. Here we have two subsystems in parallel with one feedback system and an input k. Each subsystem is described by a plant P and controller C, and the common feedback system, or load, is described by Z. The nonlinearity in this system is introduced when the maximum of the outputs from the two plants is fed back into each individual plant P as well as into the common load Z.

With the notation used throughout this chapter, x_i represents the state variables of the i^{th} subsystem (for $i = 1,2$), including both the plant and the controller of the subsystem in question. Similarly, w represents the state vector for the common load. This system can then also be described using the following state-space setup:

$$\left[\begin{array}{c} \dot{x}_1 \\ \dot{x}_2 \\ \hline \dot{w} \end{array}\right] = \left[\begin{array}{cc|c} A_d & 0 & BG \\ 0 & A_d & BG \\ \hline 0 & 0 & J \end{array}\right] \left[\begin{array}{c} x_1 \\ x_2 \\ \hline w \end{array}\right] + \left[\begin{array}{c} B_s \\ B_s \\ \hline B_L \end{array}\right] k + \left[\begin{array}{c} f_s(x) \\ f_s(x) \\ \hline f_L(x) \end{array}\right], \tag{3.31}$$

where $f_s(x)$ and $f_L(x)$ include the nonlinearity $\max(x_1, x_2)$, and A_d is dependent only upon the dynamics of the plant P and controller C.

The system matrix for this system is similar to that analyzed throughout this chapter. Recall the general setup of a system with two subsystems and one common load, ignoring input and nonlinear couplings:

$$\left[\begin{array}{c} \dot{x}_1 \\ \dot{x}_2 \\ \hline \dot{w} \end{array}\right] = \underbrace{\left[\begin{array}{cc|c} A_{Lo} + EL_dC_z & EL_qC_z & BG \\ EL_qC_z & A_{Lo} + EL_dC_z & BG \\ \hline HC & HC & J \end{array}\right]}_{A} \left[\begin{array}{c} x_1 \\ x_1 \\ \hline w \end{array}\right] \tag{3.32}$$

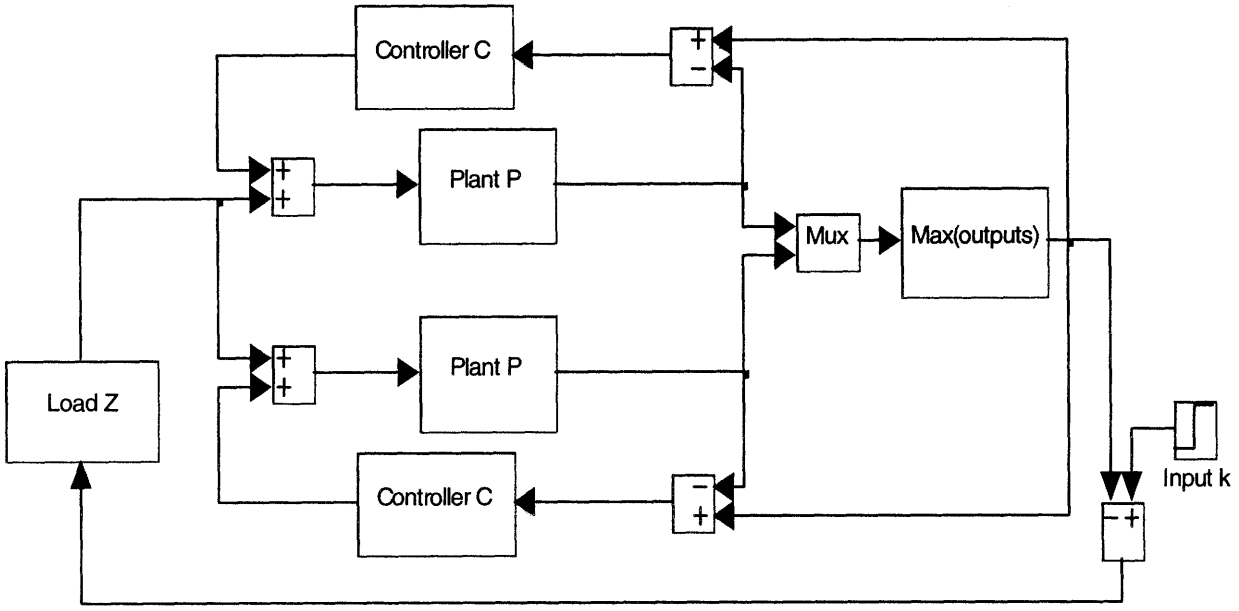

Figure 3.1: Example system with nonlinearity in the load.

Thus, in our case, $A_d = A_{Lo} + EL_dC_z$, $EL_qC_z = 0$, and $H = 0$. Also, as before, G represents the linear symmetrical influence of the common load Z on the two subsystems. Now, however, there are no linear influences from the two subsystems on the load, and thus $H = 0$. Applying the transformation T to our system yields

$$\begin{bmatrix} \dot{\tilde{x}}_1 \\ \dot{\tilde{x}}_2 \\ \dot{w} \end{bmatrix} = \left[\begin{array}{c|cc} A_d & 0 & 0 \\ \hline 0 & A_d & BG \\ 0 & 0 & J \end{array}\right] \begin{bmatrix} \tilde{x}_1 \\ \tilde{x}_2 \\ w \end{bmatrix} + \begin{bmatrix} 0 \\ B_s \\ B_L \end{bmatrix} k + \begin{bmatrix} 0 \\ \tilde{f}_s(\tilde{x}) \\ \tilde{f}_L(\tilde{x}) \end{bmatrix} \tag{3.33}$$

The matrices are now divided to show the differential- and common-mode configurations. The differential-mode is simply a linear system represented by the controller C in feedback with the plant P, as described by A_d. The common-mode is now a nonlinear system as the transformed nonlinear couplings $\tilde{f}_s(\tilde{x})$ and $\tilde{f}_L(\tilde{x})$ are functions of both the transformed state variables $\tilde{x}_1$ and $\tilde{x}_2$. It is due to this nonlinearity that the stability of the common-mode system cannot be judged simply by assessing the stability of A_d and J. Nonlinear analysis techniques must be

employed to assess the stability of such systems. In some cases, it may be possible to find Lyapunov functions to guarantee the stability of such nonlinear common-mode systems.

4 *Stability Analysis of Paralleled Converter Systems*

As discussed in the previous chapter, Lunze [1] uses linear transformations to reduce the stability analysis of a linear symmetric system consisting of N subsystems to that of a model of order twice that of the subsystem order n. We extended his analysis to include systems comprising N symmetric systems with feedback and nonlinear couplings. It was then shown that it is possible, under appropriate conditions, to reduce the stability analysis of a such a symmetric nonlinear system to that of lower-order linear and nonlinear systems; the stability of these reduced-order subsystems can be used to guarantee stability of the overall system.

As an example, we shall analyze the paralleled current-controlled converter system introduced in Chapter 2 using our extension of Lunze's analysis. A three-cell system is first analyzed and simulated, and the results for this paralleled converter system are then generalized to the N-cell case. A candidate Lyapunov function is also found.

4.1 Three-Cell Paralleled Converter System

Consider a three-cell paralleled power converter system of the type introduced in Chapter 2. The averaged circuit model for this system is shown in Figure 4.1. This system consists of three subsystems in parallel feeding into one common load.

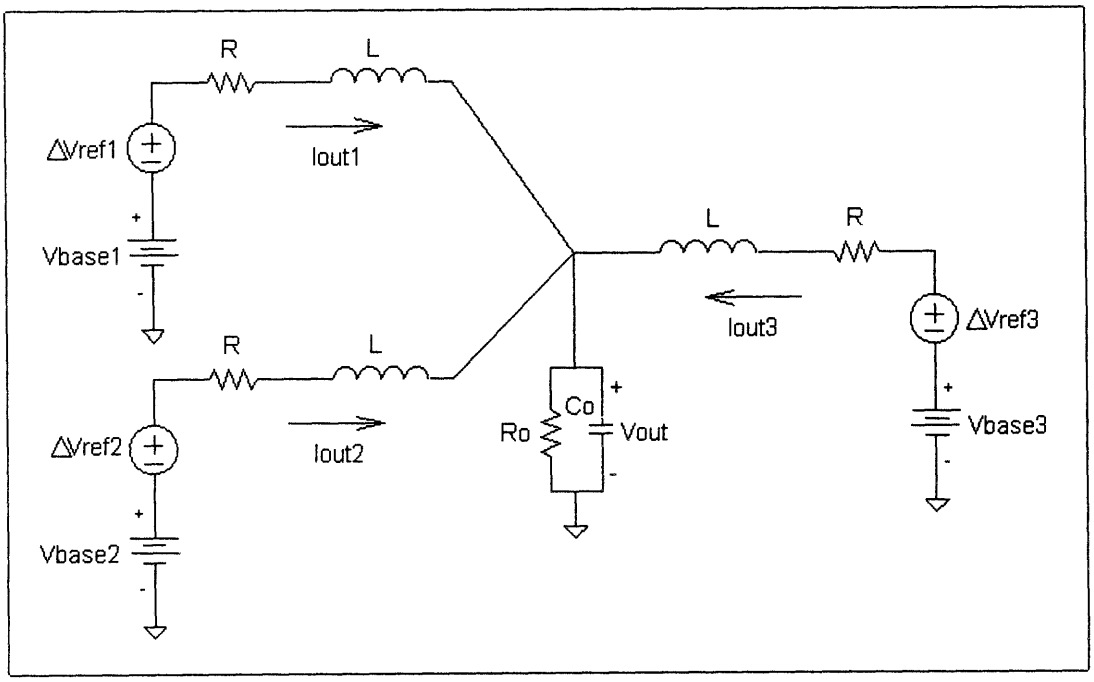

Figure 4.1: Paralleled three-cell converter system.

Recall from Chapter 2 that the state equations for the output currents, reference adjustments, and output voltage are

$$\frac{di_{outi}}{dt} = \frac{\Delta v_{refi} + V_{basei} - v_o - i_{outi}R}{L}, \tag{4.1a}$$

$$\frac{d\Delta v_{refi}}{dt} = k_1\left[i_{\max} - i_{outi}\right] - k_2\Delta v_{refi}, \tag{4.1b}$$

$$\frac{dv_o}{dt} = \frac{i_{out1} + i_{out2} + i_{out3} - \left(v_o/R_o\right)}{C_o}. \tag{4.1c}$$

for $i = 1,2,3$. Thus, each subsystem has two state variables, i_{outi} and Δv_{refi}. The feedback system has one state variable v_o. Thus, $z = \left[x_3^{\,T} \quad w^T\right]^T$ where $x_i = \left[i_{outi} \quad \Delta v_{refi}\right]^T$ and $w = v_o$.

4.1.1 Analysis

The transformation T for such a system with $N=3$, $n=2$, and $m=1$ is

$$T=\frac{1}{3}\left[\begin{array}{ccc|c} 2I & -I & -I & 0 \\ -I & 2I & -I & 0 \\ I & I & I & 0 \\ \hline 0 & 0 & 0 & 3 \end{array}\right], \tag{4.2}$$

where the identity matrices I are 2×2. Thus, our new state variables are defined as

$$i_{x1}=\frac{2i_{out1}-i_{out2}-i_{out3}}{3} \tag{4.3a}$$

$$v_{x1}=\frac{2\Delta v_{ref1}-\Delta v_{ref2}-\Delta v_{ref3}}{3} \tag{4.3b}$$

$$i_{x2}=\frac{-i_{out1}+2i_{out2}-i_{out3}}{3} \tag{4.3c}$$

$$v_{x2}=\frac{-\Delta v_{ref1}+2\Delta v_{ref2}-\Delta v_{ref3}}{3} \tag{4.3d}$$

$$i_{y}=\frac{i_{out1}+i_{out2}+i_{out3}}{3} \tag{4.3e}$$

$$v_{y}=\frac{\Delta v_{ref1}+\Delta v_{ref2}+\Delta v_{ref3}}{3} \tag{4.3f}$$

$$v_{o}=v_{o} \tag{4.3g}$$

The state evolution equations are now given by

$$\frac{di_{x1}}{dt}=\frac{3v_{x1}+\left(2V_{base1}-V_{base2}-V_{base3}\right)-3i_{x1}R}{3L} \tag{4.4a}$$

$$\frac{dv_{x1}}{dt}=-k_1 i_{x1}-k_2 v_{x1} \tag{4.4b}$$

$$\frac{di_{x2}}{dt}=\frac{3v_{x2}+\left(-V_{base1}+2V_{base2}-V_{base3}\right)-3i_{x2}R}{3L} \tag{4.4c}$$

$$\frac{dv_{x2}}{dt} = -k_1 i_{x2} - k_2 v_{x2} \tag{4.4d}$$

$$\frac{di_y}{dt} = \frac{3v_y + \left(V_{base1} + V_{base2} + V_{base3}\right) - 3v_o - 3i_y R}{3L} \tag{4.4e}$$

$$\frac{dv_y}{dt} = k_1 \underbrace{\left(i_{\max} - i_y\right)}_{\tilde{f}} - k_2 v_y \tag{4.4f}$$

$$\frac{dv_o}{dt} = \frac{3i_y - \left(v_o / R_o\right)}{C_o} \tag{4.4g}$$

The transformed function $\tilde{f}$ can be defined as

$$\tilde{f} = \begin{cases} \left|i_{x1}\right|, & \text{if } i_{\max} = i_{out1} \\ \left|i_{x2}\right|, & \text{if } i_{\max} = i_{out2} \\ \left|i_{x1} + i_{x2}\right|, & \text{if } i_{\max} = i_{out3} \end{cases} \tag{4.5}$$

These equations can be physically represented by the circuits shown in Figure 4.2 and Figure 4.3. In these figures, $\tilde{f}$ is as defined above, and

$$C_x = C_y = \frac{1}{k_1} \text{ and } R_x = R_y = \frac{k_1}{k_2}.$$

For stability analysis, it is only necessary to assess the stability of one of the (identical) differential-mode circuits, along with the common-mode circuit. The differential-mode circuits are linear, and the nonlinearity of the system is simply captured in the current source of the common-mode circuit. The load appears only in the common-mode configuration as well. The beauty of this transformation is the fact that the common-mode circuit variables do not feed back into the differential-mode circuits. Because we know that the differential-mode circuits are stable, we know that i_{x1} and i_{x2} decay exponentially to their respective operating points. Thus, the common-mode circuit is stable as well. Since the circuit models of Figure 4.2 and Figure 4.3

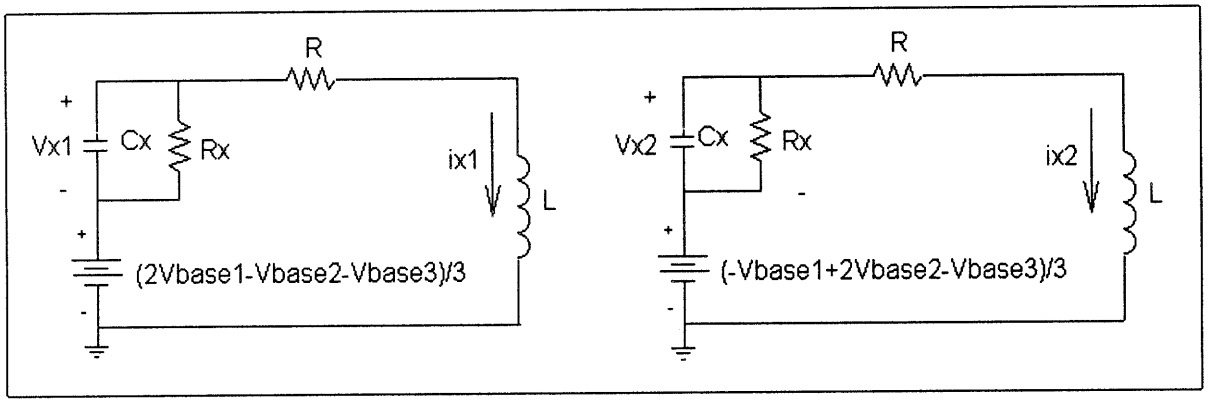

Figure 4.2: Differential-mode circuit configurations of a three-cell system.

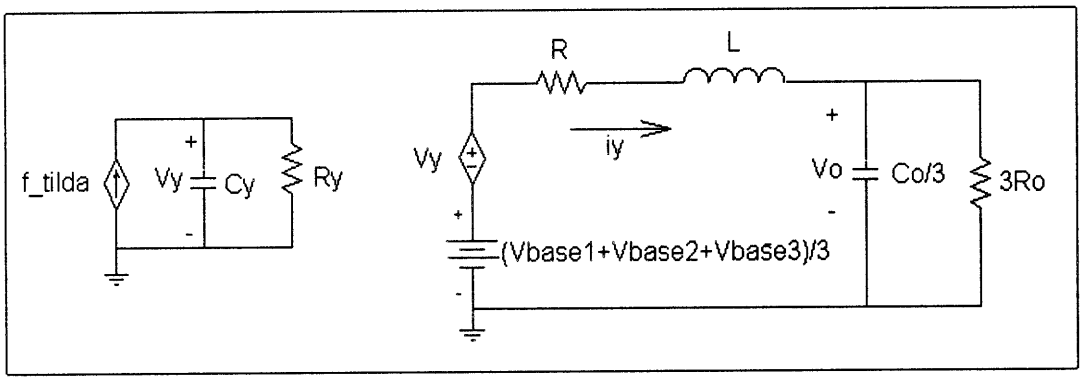

Figure 4.3: Common-mode circuit configuration of a three-cell system.

are stable, the original paralleled three-cell current-mode-controlled power converter system is also stable[1].

Note also that a Lyapunov function for this system can be chosen as the energy in the active elements in the common- and differential-mode configurations.

[1] This circuit-based analysis is due to Dr. David Perreault, and significantly helped our understanding of the implications of transformation to differential- and common-mode subsystems.

4.1.2 Simulation

Consider the simulation of this three-cell paralleled converter system. We will assume that the control gains on Δv_{refi} are given by $k_1 = 5$, $k_2 = 2$, the output impedance of each converter is given by $L = 0.03H$, $R = 4\Omega$, and the load is given by $C_o = 0.05F$, $R_o = 1\Omega$. Also, we will assume that $V_{base1} = 0\,\text{V}$, $V_{base2} = 0.1\,\text{V}$, and $V_{base3} = 0.05\,\text{V}$, and that the initial conditions on the reference voltages Δv_{refi}, for $i = 1,2,3$, are given by 0.5, 0.2 and 0 volts respectively. The simulated response of the three-cell system for the specified parameters and initial conditions is given in Figure 4.4.

The switching action of the nonlinear 'max' coupling can be seen at time 0.45, where the current of the second converter overtakes that of the first converter. Note that in steady state, i_{out2} is maximum, and thus the steady state value of v_{ref2} is zero. The other reference voltages settle out to their respective operating points as $t \to \infty$.

Now, we would like to piece together these waveforms from the differential- and common-mode configurations obtained by applying the similarity transformation T. The circuit diagrams for these two configurations are shown in Figure 4.2 and Figure 4.3, and their corresponding simulation setups are shown in Figure 4.5 and Figure 4.6. In the differential-mode simulation setup,

$$V_{basex1} = \frac{2V_{base1} - V_{base2} - V_{base3}}{3} = -0.05\,\text{V} \text{ and } V_{basex2} = \frac{-V_{base1} + 2V_{base2} - V_{base3}}{3} = 0.05\,\text{V}.$$

Similarly for the common-mode, the reference base voltage V_{basey} is the average of the three reference base voltages, or 0.05 volts. The initial conditions on the integrators are determined in an identical fashion. Thus, for the two differential-modes, the initial conditions are 0.2667 and -0.0333 volts respectively. For the common-mode, the initial condition on the integrator is the average of the original three initial conditions, or 0.2333 volts. Also, the load in the common-mode configuration is given by a resistance of $3R_o$ in parallel with a capacitance of $C_o/3$. Note that the input $\tilde{f}$ in the common-mode is a function of the differential-mode currents i_{x1} and i_{x2}, as defined in the previous section.

It is now possible to piece together the waveforms of our original system from the waveforms obtained from the differential- and common-mode systems. For example, from the definitions of i_y, i_{x1}, v_y and v_{x2}, we know that $i_y + i_{x1} = i_{out1}$ and $v_y + v_{x2} = v_{ref2}$. Also, we know that the output voltage v_o of our original system should equal the output voltage v_{oy} obtained from the common-mode system. These three waveforms are shown in Figure 4.7. All other output current and reference voltage waveforms can be obtained through similar linear combinations of the differential- and common-mode variables. These simulations confirm our theoretical results.

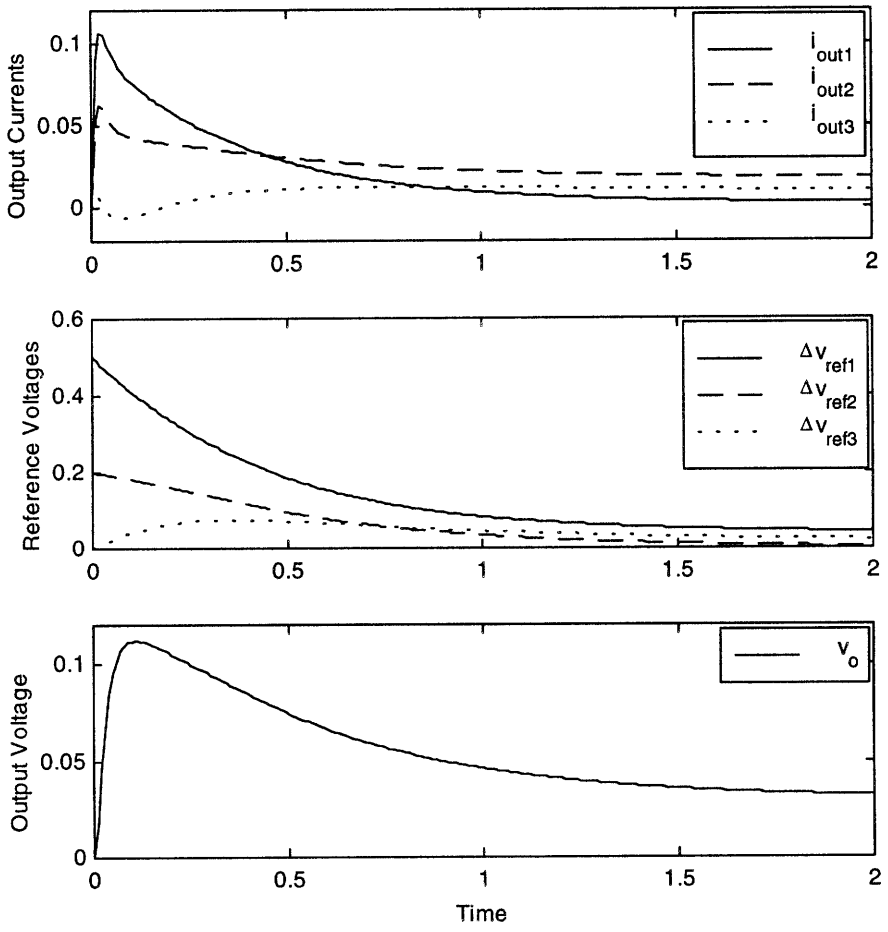

Figure 4.4: Paralleled three-cell converter system simulation.

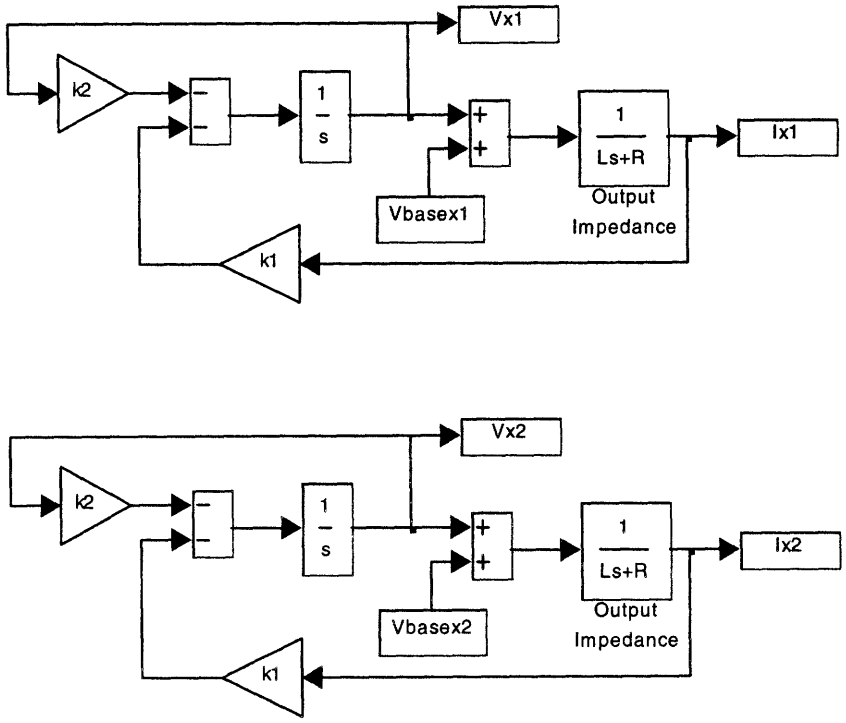

Figure 4.5: Differential-mode simulation setup of a three-cell converter system.

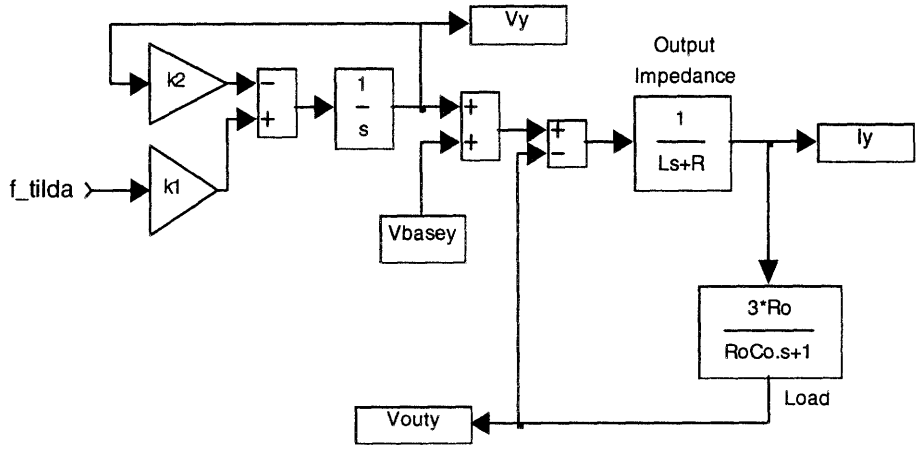

Figure 4.6: Common-mode simulation setup of a three-cell converter system

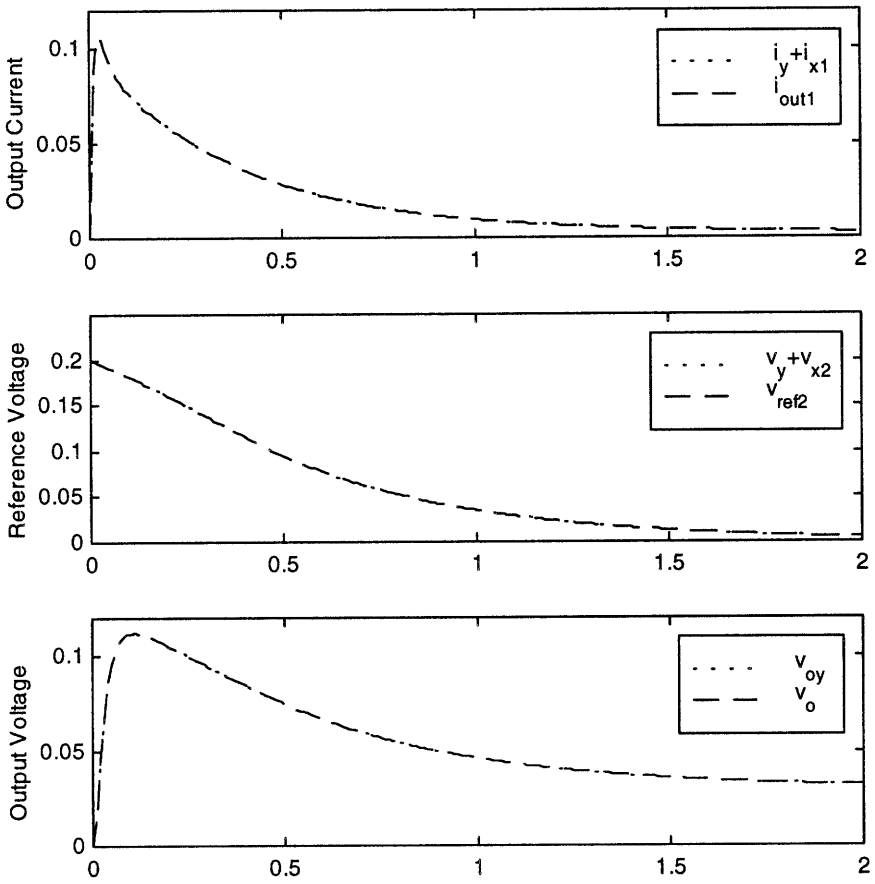

Figure 4.7: Responses from the original system and as reconstructed from the transformed system for a three-cell converter system.

4.2 *N*-cell Paralleled Converter System

Now let's consider an *N*-cell paralleled converter system of this type. For the *N*-cell system, the state equations can be generalized to

$$\frac{di_{outi}}{dt} = \frac{\Delta v_{refi} + V_{basei} - v_o - i_{outi}R}{L}, \tag{4.6a}$$

$$\frac{d\Delta v_{refi}}{dt} = k_1\left(i_{\max} - i_{outi}\right) - k_2\Delta v_{refi}, \tag{4.6b}$$

$$\frac{dv_o}{dt} = \frac{1}{C_o}\left[\sum_{j=1}^{N} i_{outj} - \frac{v_o}{R_o}\right], \tag{4.6c}$$

for $i = 1,2,..,N$. Letting $x_i = \begin{bmatrix} i_{outi} & \Delta v_{refi} \end{bmatrix}^T$ and $w = v_o$, we rewrite the state equations in matrix form as follows:

$$\left[\begin{array}{c} \dot{x}_1 \\ \dot{x}_2 \\ \vdots \\ \dot{x}_N \\ \hline \dot{w} \end{array}\right] = \left[\begin{array}{cccc|c} A_d & 0 & \cdots & 0 & BG \\ 0 & A_d & \cdots & 0 & BG \\ \vdots & \vdots & & \vdots & \vdots \\ 0 & 0 & \cdots & A_d & BG \\ \hline HC & HC & \cdots & HC & J \end{array}\right]\left[\begin{array}{c} x_1 \\ x_2 \\ \vdots \\ x_N \\ \hline w \end{array}\right] + \left[\begin{array}{c} B_1 \\ B_2 \\ \vdots \\ B_N \\ \hline 0 \end{array}\right] + \left[\begin{array}{c} f \\ f \\ \vdots \\ f \\ \hline 0 \end{array}\right] \tag{4.7}$$

where

$$A_d = \begin{bmatrix} -R/L & 1/L \\ -k_1 & -k_2 \end{bmatrix}, \quad BG = \begin{bmatrix} -1/L \\ 0 \end{bmatrix}, \quad CH = \begin{bmatrix} 1/C_o & 0 \end{bmatrix},$$

$$J = \frac{-1}{R_o C_o}, \quad B_i = \begin{bmatrix} V_{basei}/L \\ 0 \end{bmatrix}, \quad f = \begin{bmatrix} 0 \\ k_1 \cdot \max\limits_j\left(i_{outj}\right) \end{bmatrix}.$$

The transformation T for this system, as introduced in the previous chapter, is

$$T=\frac{1}{N}\left[\begin{array}{ccccc|c} (N-1)I & -I & \cdots & -I & -I & 0 \\ -I & (N-1)I & \cdots & -I & -I & 0 \\ \vdots & \vdots & & \vdots & \vdots & \vdots \\ -I & -I & \cdots & (N-1)I & -I & 0 \\ I & I & \cdots & I & I & 0 \\ \hline 0 & 0 & \cdots & 0 & 0 & N \end{array}\right] \tag{4.8}$$

Using this transformation, we arrive at our new state variable block vector as shown below:

$$T\left[\frac{x}{w}\right]=\frac{1}{N}\left[\begin{array}{ccccc|c} (N-1)I & -I & \cdots & -I & -I & 0 \\ -I & (N-1)I & \cdots & -I & -I & 0 \\ \vdots & \vdots & & \vdots & \vdots & \vdots \\ -I & -I & \cdots & (N-1)I & -I & 0 \\ I & I & \cdots & I & I & 0 \\ \hline 0 & 0 & \cdots & 0 & 0 & N \end{array}\right]\left[\begin{array}{c} x_1 \\ x_2 \\ \vdots \\ x_{N-1} \\ x_N \\ \hline w \end{array}\right]=\left[\begin{array}{c} \tilde{x}_1 \\ \tilde{x}_2 \\ \vdots \\ \tilde{x}_{N-1} \\ \tilde{x}_N \\ \hline w \end{array}\right]=\left[\frac{\tilde{x}}{w}\right], \tag{4.9}$$

where $\tilde{x}_i=\begin{bmatrix} i_{xi} & v_{xi} \end{bmatrix}^T$, $\tilde{x}_N=\begin{bmatrix} i_y & v_y \end{bmatrix}^T$ and $w=v_o$, for $i=1,2,..,(N-1)$.

The overall transformed system is then defined by

$$\left[\begin{array}{c} \dot{\tilde{x}}_1 \\ \dot{\tilde{x}}_2 \\ \vdots \\ \dot{\tilde{x}}_N \\ \hline \dot{w} \end{array}\right]=T\left[\begin{array}{ccccc|c} A_d & 0 & \cdots & 0 & BG \\ 0 & A_d & \cdots & 0 & BG \\ \vdots & \vdots & & \vdots & \vdots \\ 0 & 0 & \cdots & A_d & BG \\ \hline HC & HC & \cdots & HC & J \end{array}\right]T^{-1}\left[\begin{array}{c} \tilde{x}_1 \\ \tilde{x}_2 \\ \vdots \\ \tilde{x}_N \\ \hline w \end{array}\right]+T\left[\begin{array}{c} B_1 \\ B_2 \\ \vdots \\ B_N \\ \hline 0 \end{array}\right]+T\left[\begin{array}{c} f \\ f \\ \vdots \\ f \\ \hline 0 \end{array}\right]$$

$$= \left[\begin{array}{ccccc|c} A_d & 0 & \cdots & 0 & 0 & 0 \\ 0 & A_d & \cdots & 0 & 0 & 0 \\ \vdots & \vdots & & \vdots & \vdots & \vdots \\ 0 & 0 & \cdots & A_d & 0 & 0 \\ 0 & 0 & \cdots & 0 & A_c & BG \\ \hline 0 & 0 & \cdots & 0 & NHC & J \end{array}\right]\left[\begin{array}{c} \tilde{x}_1 \\ \tilde{x}_2 \\ \vdots \\ \tilde{x}_{N-1} \\ \tilde{x}_N \\ \hline w \end{array}\right] + \left[\begin{array}{c} \tilde{B}_1 \\ \tilde{B}_2 \\ \vdots \\ \tilde{B}_{N-1} \\ \tilde{B}_N \\ \hline 0 \end{array}\right] + \left[\begin{array}{c} 0 \\ 0 \\ \vdots \\ 0 \\ \tilde{f} \\ \hline 0 \end{array}\right] \tag{4.10}$$

where, as defined earlier,

$$A_d = \begin{bmatrix} -R/L & 1/L \\ -k_1 & -k_2 \end{bmatrix},\quad BG = \begin{bmatrix} -1/L \\ 0 \end{bmatrix},\quad CH = \begin{bmatrix} 1/C_o & 0 \end{bmatrix},\ \text{and}\ J = \frac{-1}{R_o C_o}.$$

Also, for $i = 1,2,..,(N-1)$,

$$\tilde{B}_i = \frac{1}{NL}\begin{bmatrix} (N-1)V_{basei} - \sum_{\substack{j=1 \\ j\neq i}}^{N} V_{basej} \\ 0 \end{bmatrix} \text{ and } \tilde{B}_N = \begin{bmatrix} \frac{1}{NL}\sum_{j=1}^{N} V_{basej} \\ 0 \end{bmatrix}.$$

The question now arises as to the values of A_c and $\tilde{f}$. Before we address this issue, however, recall that the matrix A_d represents the $(N-1)$ identical differential-mode configurations of the system, and the matrix A_{cc} represents the common-mode configuration, where

$$A_{cc} = \begin{bmatrix} A_c & BG \\ HC & J \end{bmatrix}. \tag{4.11}$$

The transformation T transforms and isolates the nonlinearity f of the original system into the common-mode configuration. The stability of the system rests upon the stability of the differential- and common-mode configurations.

Now, there are many possibilities for representing the values of A_c and $\tilde{f}$, of which we will consider two. These are discussed in the following subsections.

4.2.1 Isolating The 'Max' Nonlinearity

The first possibility for A_c and $\tilde{f}$, which falls directly out of the transformation T, is

$$A_c = A_d = \begin{bmatrix} -R/L & 1/L \\ -k_1 & -k_2 \end{bmatrix} \tag{4.12}$$

and

$$\tilde{f} = \begin{bmatrix} 0 \\ k_1 \cdot \max_j \left(i_{outj} \right) \end{bmatrix} \tag{4.13}$$

where the 'max' nonlinearity is expressed as a function of the original state variables. This form reveals the effectiveness of the similarity transformation T in isolating the 'max' nonlinearity to the common-mode configuration.

Let us check our results for the N-cell paralleled power converter example from the general results discussed in the previous chapter. Recall the form of the nonlinearity vector F for the original system with feedback:

$$F = \begin{bmatrix} f_{N1}(\tilde{x}_1, \tilde{x}_2, .., \tilde{x}_N) \\ f_{N1}(\tilde{x}_1, \tilde{x}_2, .., \tilde{x}_N) + f_2(\tilde{x}_1) \\ f_{N1}(\tilde{x}_1, \tilde{x}_2, .., \tilde{x}_N) + f_3(\tilde{x}_1, \tilde{x}_2) \\ \vdots \\ f_{N1}(\tilde{x}_1, \tilde{x}_2, .., \tilde{x}_N) + f_{N-1}(\tilde{x}_1, \tilde{x}_2, .., \tilde{x}_{N-2}) \\ f_{N1}(\tilde{x}_1, \tilde{x}_2, .., \tilde{x}_N) - \sum_{i=1}^{N-1} f_i(\tilde{x}_1, \tilde{x}_2, .., \tilde{x}_{i-1}) \\ f_{N2}(\tilde{x}_1, \tilde{x}_2, .., \tilde{x}_N) \end{bmatrix} \tag{4.14}$$

Note that f_{Ni} is not only a function of the transformed state variables $\tilde{x}_1$ through $\tilde{x}_{N-1}$, but of $\tilde{x}_N$ as well. Thus, the common-mode configuration of this system will be a nonlinear system, as discussed at the end of the previous chapter.

The nonlinearity vector for our example before the transformation is $[f \quad f \quad f \quad \cdots \quad f \mid f \quad 0]$. Comparing these two forms reveals that, for $i = 1,2,..,(N-1)$,

$$f_i(\tilde{x}_1, \tilde{x}_2, .., \tilde{x}_{i-1}) = 0 \tag{4.15a}$$

$$f_{N2}(\tilde{x}_1, \tilde{x}_2, .., \tilde{x}_N) = 0 \tag{4.15b}$$

$$f_{N1}(\tilde{x}_1, \tilde{x}_2, .., \tilde{x}_N) = f = \begin{bmatrix} 0 \\ k_1 i_{\max}(x) \end{bmatrix}. \tag{4.15c}$$

As expected, the transformation T transforms and isolates the nonlinearity f of the original system into the common-mode configuration.

4.2.2 Stability Analysis

In order to further simplify the analysis required to assess the stability of the nonlinear common-mode system, we can adjust the description of the nonlinear common-mode system. We now express A_c as

$$A_c = \begin{bmatrix} -R/L & 1/L \\ 0 & -k_2 \end{bmatrix}. \tag{4.16}$$

In this case, as in the three-cell case, the nonlinearity becomes

$$\tilde{f} = \begin{bmatrix} 0 \\ \max_j\left(i_{outj}\right) - i_y \end{bmatrix}. \tag{4.17a}$$

Simplifying, we can express $\tilde{f}$ as rectified versions of the combinations of the differential-mode currents i_{xi}, i.e.

$$\tilde{f} = \begin{cases} \begin{bmatrix} 0 \\ |i_{xi}| \end{bmatrix}, & \text{if } \max_j\left(i_{outj}\right) = i_{outi}, \text{ for } i = 1,2,..,(N-1) \\ \begin{bmatrix} 0 \\ \left|\sum_{i=1}^{N-1} i_{xi}\right| \end{bmatrix}, & \text{if } \max_j\left(i_{outj}\right) = i_N \end{cases} \tag{4.17b}$$

This form is more convenient from a stability standpoint because it not only restricts the nonlinearity to the common-mode subsystem, but also destroys any feedback from the common-mode subsystem to the differential-mode subsystems.

This form also allows us to easily express the transformed system in terms of circuit diagrams. The setup results in $(N-1)$ differential-mode circuits, of which only one needs to be analyzed to assess stability, and a common-mode circuit (Figure 4.8 and Figure 4.9). In these figures,

$$C_x = C_y = \frac{1}{k_1}, \quad R_x = R_y = \frac{k_1}{k_2}, \text{ and } V_{baserefs} = \frac{1}{N}\left[(N-1)V_{basei} - \sum_{\substack{j=1 \\ j\neq i}}^{N} V_{basej}\right].$$

for $i = 1,2,..,(N-1)$. In this case, the linear differential-mode circuit is obviously stable, and thus the switching current source on the common-mode circuit decays exponentially to a constant value, making the common-mode circuits stable as well. Thus, the overall system is stable.

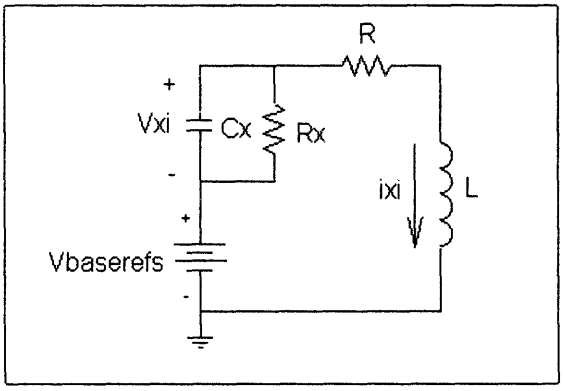

Figure 4.8: Differential-mode circuit configuration of an *N*-cell system.

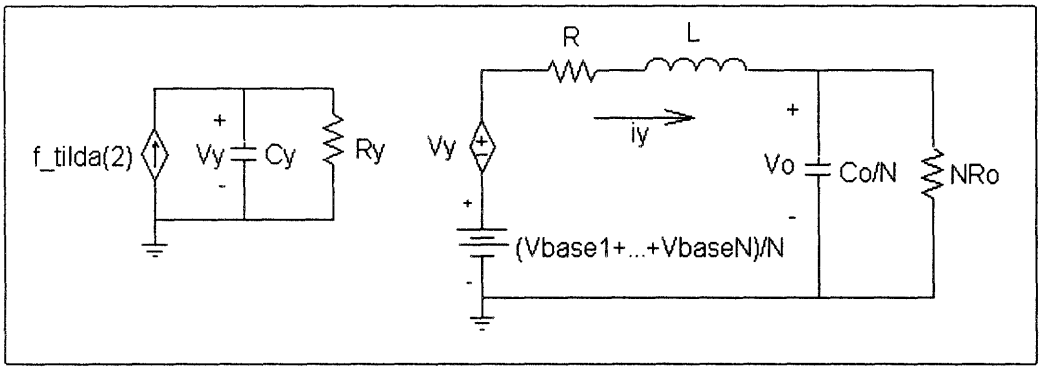

Figure 4.9: Common-mode circuit configuration of an *N*-cell system.

Note that one Lyapunov function V for the N-cell system with load dynamics is simply the energy stored in the active elements of the differential- and common-mode circuit configurations. Thus,

$$V = \frac{1}{2}C_x v_{xi}^2 + \frac{1}{2}Li_{xi}^2 + \frac{1}{2}C_y v_y^2 + \frac{1}{2}Li_y^2 + \frac{1}{2N}C_o v_o^2, \tag{4.18}$$

for $i = 1,2,..,(N-1)$, and $C_x = C_y = 1/k_1$. Of course, this Lyapunov function V can be written in terms of the reference voltages and the output currents by making a simple substitution as dictated by the similarity transformation T. This Lyapunov function guarantees the decay of the state variables to their respective operating points.

5 *Piecewise Quadratic Lyapunov Functions*

Some symmetrically-coupled systems with nonlinear feedback can be modeled as hybrid systems, and thus tools developed to examine such systems can be employed. The paralleled current-mode-controlled power converters with 'max' current sharing controls, discussed in Chapter 2, are merely two examples of nonlinear feedback systems that can be modeled in this fashion. One method of examining such hybrid systems is given by Johansson and Rantzer [2]. In this chapter, we will employ their approach to analyze the two paralleled converter models of Chapter 2. This will allow us to assess the strengths and weaknesses of the approach in a practical context.

5.1 Background

Johansson and Rantzer provide insight into finding Lyapunov functions to guarantee the stability of nonlinear systems that have piecewise affine dynamics [2]. Such systems exist naturally as hybrid control systems and as approximations to other nonlinear systems, to cite only two examples. They first partition the state-space of a piecewise affine system into a number of closed cells, and then search for a piecewise continuous Lyapunov function for the system. The piecewise system analysis described by Johansson and Rantzer is employed below.

5.1.1 System Setup

Consider the analysis of a piecewise affine system defined by

$$\dot{x} = A_i x + a_i \tag{5.1}$$

for $x \in X_i$ and $i \in I$, where X_i is the partition of the state-space into a number of polytopic cells. For notational convenience, we first introduce

$$\overline{A}_i = \begin{bmatrix} A_i & a_i \\ 0 & 0 \end{bmatrix}, \qquad i \in I. \tag{5.2}$$

We now construct matrices $\overline{E}_i = \begin{bmatrix} E_i & e_i \end{bmatrix}$ such that the i^{th} cell is characterized by

$$\overline{E}_i \begin{bmatrix} x \\ 1 \end{bmatrix} \geq 0, \qquad x \in X_i, \qquad i \in I, \tag{5.3}$$

where the vector inequality is to be interpreted component-wise. We also construct matrices $\overline{F}_i = \begin{bmatrix} F_i & f_i \end{bmatrix}$ such that the behavior in the boundary between cells i and j is characterized by

$$\overline{F}_i \begin{bmatrix} x \\ 1 \end{bmatrix} = \overline{F}_j \begin{bmatrix} x \\ 1 \end{bmatrix}, \qquad x \in X_i \text{ and } X_j \qquad i, j \in I. \tag{5.4}$$

As will be shown below, the matrices $\overline{F}_i$ are used to ensure continuity of the Lyapunov function across cell boundaries [2].

5.1.2 S-Procedure

The established approach [5] of finding a global quadratic Lyapunov function

$$V(x) = x^T P x, \tag{5.5}$$

for piecewise affine systems is possible if there exists a common symmetric, positive definite matrix P obtained by simultaneously solving the matrix inequalities

$$A_i^T P + P A_i < 0, \qquad \text{for } i \in I, \tag{5.6}$$

where the inequality is now in the sense of positive definiteness. This method fails for many cases, however, because it is unnecessarily conservative. Because the dynamics of A_i only apply within cell X_i for a piecewise affine system, we need only require that

$$x^T\left(A_i^T P + PA_i\right)x < 0, \text{ for } x \in X_i. \tag{5.7}$$

We now introduce symmetric matrices S_i such that $x^T S_i x \geq 0$ for $x \in X_i$, to obtain the relaxed stability conditions

$$A_i^T P + PA_i + S_i < 0. \tag{5.8}$$

This method of introducing flexibility into the stability conditions is called the *S*-procedure [2].

From the description given previously for the piecewise affine system, it is simple to construct matrices for use in the *S*-procedure. If U_i is a symmetric matrix with non-negative entries, then

$$\begin{bmatrix} x \\ 1 \end{bmatrix}^T \underbrace{\overline{E}_i^T U_i \overline{E}_i}_{\overline{S}_i} \begin{bmatrix} x \\ 1 \end{bmatrix} \geq 0, \quad x \in X_i, \qquad i \in I. \tag{5.9}$$

5.1.3 *Johansson and Rantzer's Theorem for Piecewise Quadratic Stability*

It follows that for the stability of general piecewise affine systems, we can search for Lyapunov functions of the form

$$V(x) = \begin{bmatrix} x \\ 1 \end{bmatrix}^T \overline{P}_i \begin{bmatrix} x \\ 1 \end{bmatrix}, \quad x \in X_i, \qquad i \in I. \tag{5.10}$$

Note that this Lyapunov function is required to be continuous across cell boundaries. Sufficient conditions for the existence of such a piecewise quadratic Lyapunov function are described below.

Consider symmetric matrices T, U_i and W_i, where $i \in I$, and U_i and W_i have non-negative entries. If there exist matrices

$$\overline{P}_i = \overline{F}_i^T T \overline{F}_i \tag{5.11}$$

such that

$$0 > \overline{A}_i^T \overline{P}_i + \overline{P}_i \overline{A}_i + \overline{E}_i^T U_i \overline{E}_i \,, \tag{5.12a}$$

$$0 < \overline{P}_i - \overline{E}_i^T W_i \overline{E}_i \tag{5.12b}$$

then $x(t)$ tends to zero exponentially [2].

5.2 Analysis of Paralleled Power Converters

In order to simplify the analysis, the models that will be studied are those of the dual-cell converter systems discussed in Chapter 2 with load dynamics eliminated. Recall that in this case, the load can be modeled as a constant current source I_{out}. For convenience, we let $I_{out} = 0$, i.e. $i_{out2} = -i_{out1}$, and thus the maximum current can be represented by the absolute value of output current of either converter. Recall also that a constant output current of zero does not affect the transient response of this system. If this current was some nonzero constant value, it would merely introduce an offset into the analysis.

A Piecewise Linear (PWL) Toolbox, written by Johansson and Rantzer, was obtained to perform all the simulations in the following sections [3]. The PWL toolbox is an interface to the `Linear Matrix Inequality (LMI) Control Toolbox` in `MATLAB` [4]. The modifications made to the PWL Toolbox and samples of the code used to obtain the various results for this chapter are given in Appendix B.

5.2.1 Analysis of Dual-Cell Converter Model

Recall the setup for the paralleled dual-cell current-mode-controlled power converter system as introduced in Chapter 2, repeated here as Figure 5.1. Including both offsets and proportional decay terms, the state equations for the converter output currents and reference voltages are

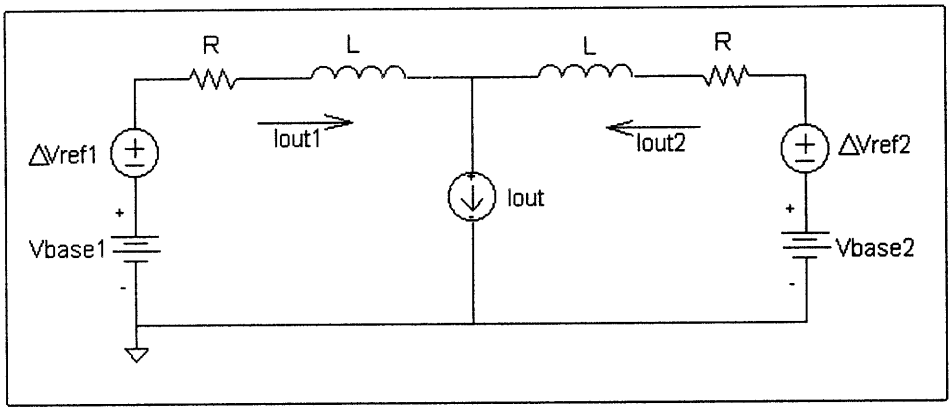

Figure 5.1: Averaged circuit model of a dual-cell converter system.

$$\frac{di_{outi}}{dt} = \frac{\Delta v_{refi} + V_{basei} - v_o - i_{outi}R}{L}, \tag{5.13a}$$

$$\frac{d\Delta v_{refi}}{dt} = k_1\left[i_{\max} - i_{outi}\right] - k_2\Delta v_{refi} \tag{5.13b}$$

for $i = 1,2$. In the absence of load dynamics, i.e. where $i_{out2} = -i_{out1}$, it is unnecessary to keep both the output currents as our state variables. Thus, we introduce the difference of the two output currents as a new state variable i_d, i.e. $i_d = i_{out1} - i_{out2}$. Then

$$\frac{di_d}{dt} = \frac{2\left(\Delta v_{ref1} - \Delta v_{ref2}\right) + 2\left(V_{base1} - V_{base2}\right) - i_d R_{eq}}{L_{eq}}, \tag{5.14}$$

where $L_{eq} = 2L$, and $R_{eq} = 2R$. Also, we can rewrite the state equations for the reference voltages as follows:

$$\left.\begin{aligned} \frac{d\Delta v_{ref1}}{dt} &= -k_2\Delta v_{ref1} \\ \frac{d\Delta v_{ref2}}{dt} &= k_1 i_d - k_2\Delta v_{ref2} \end{aligned}\right\} \text{ for } i_{\max} = i_{out1} \Leftrightarrow i_d > 0 \tag{5.15a}$$

$$\left.\begin{aligned}\frac{d\Delta v_{ref1}}{dt} &= -k_1 i_d - k_2 \Delta v_{ref1} \\ \frac{d\Delta v_{ref2}}{dt} &= -k_2 \Delta v_{ref2}\end{aligned}\right\} \text{ for } i_{\max} = i_{out2} \Leftrightarrow i_d < 0 \tag{5.15b}$$

The division in state-space for this system is thus based upon the sign of i_d; the two regions in our state-space are given by $i_d > 0$ and $i_d < 0$.

Because this system has a nonzero operating point, and the theorem by Johansson and Rantzer assumes that the equilibrium point occurs where all the state variables are zero, we redefine our state variables from i_d, Δv_{ref1} and Δv_{ref2} to

$$\underbrace{\begin{bmatrix}\tilde{i}_d \\ \Delta\tilde{v}_{ref1} \\ \Delta\tilde{v}_{ref2}\end{bmatrix}}_{\tilde{x}} = \begin{bmatrix}i_d - I_d \\ \Delta v_{ref1} - V_{ref1} \\ \Delta v_{ref2} - V_{ref2}\end{bmatrix}, \tag{5.16}$$

where the operating point, found by simply setting all derivatives to zero, is given by

$$V_{ref1} = 0, \tag{5.17a}$$

$$V_{ref2} = \frac{2k_1\left(V_{base1} - V_{base2}\right)}{2k_1 + k_2 R_{eq}}, \tag{5.17b}$$

$$I_d = \frac{k_2 V_{ref2}}{2k_1} \tag{5.17c}$$

for $V_{base1} > V_{base2}$. There is a similar operating point for the case where $V_{base2} > V_{base1}$. The new state equations for our system now become

$$\frac{d\tilde{i}_d}{dt} = \frac{2\left(\Delta\tilde{v}_{ref1} + V_{ref1} - \Delta\tilde{v}_{ref2} - V_{ref2}\right) + 2\left(V_{base1} - V_{base2}\right) - \left(\tilde{i}_d + I_d\right)R_{eq}}{L_{eq}}, \tag{5.18a}$$

$$\left.\begin{aligned}\frac{d\Delta\tilde{v}_{ref1}}{dt} &= -k_2\left(\Delta\tilde{v}_{ref1} + V_{ref1}\right)\\ \frac{d\Delta\tilde{v}_{ref2}}{dt} &= k_1\left(\tilde{i}_d + I_d\right) - k_2\left(\Delta\tilde{v}_{ref2} + V_{ref2}\right)\end{aligned}\right\} \text{ for } i_{\max} = i_{out1} \Leftrightarrow \tilde{i}_d + I_d > 0 \qquad (5.18b)$$

$$\left.\begin{aligned}\frac{d\Delta\tilde{v}_{ref1}}{dt} &= -k_1\left(\tilde{i}_d + I_d\right) - k_2\left(\Delta\tilde{v}_{ref1} + V_{ref1}\right)\\ \frac{d\Delta\tilde{v}_{ref2}}{dt} &= -k_2\left(\Delta\tilde{v}_{ref2} + V_{ref2}\right)\end{aligned}\right\} \text{ for } i_{\max} = i_{out2} \Leftrightarrow \tilde{i}_d + I_d < 0 \qquad (5.18c)$$

The divisions in our state-space are now determined by the value of $\tilde{i}_d$. Using the notation

$$\dot{\tilde{x}} = A_i\tilde{x} + a_i \qquad (5.19)$$

and constructing matrices $\overline{E}_i$ and $\overline{F}_i$ such that

$$\overline{E}_i\begin{bmatrix}\tilde{x}\\ 1\end{bmatrix} \geq 0 \quad \text{for } \tilde{x} \in \text{Region } i, \qquad (5.20a)$$

$$\overline{F}_1\begin{bmatrix}\tilde{x}\\ 1\end{bmatrix} = \overline{F}_2\begin{bmatrix}\tilde{x}\\ 1\end{bmatrix} \quad \text{for } \tilde{x} \in \text{Region 1 and Region 2} \qquad (5.20b)$$

for $i = 1,2$, we arrive at the region specifications given in Table 5.1.

The code *noload.m* used to set up and simulate this system using the modified PWL software [3] is given in Appendix B. Despite the fact that we found a quadratic Lyapunov function to guarantee stability of this system in the previous chapter, the software does not find a piecewise quadratic Lyapunov function for this case.

Table 5.1: State-space description for the dual-cell converter model

Region 1: $\tilde{i}_d > -I_d$	**Region 2:** $\tilde{i}_d < -I_d$
$A_1 = \begin{bmatrix} \frac{-R_{eq}}{L_{eq}} & \frac{2}{L_{eq}} & \frac{-2}{L_{eq}} \\ 0 & -k_2 & 0 \\ k_1 & 0 & -k_2 \end{bmatrix}$	$A_2 = \begin{bmatrix} \frac{-R_{eq}}{L_{eq}} & \frac{2}{L_{eq}} & \frac{-2}{L_{eq}} \\ -k_1 & -k_2 & 0 \\ 0 & 0 & -k_2 \end{bmatrix}$
$a_1 = \begin{bmatrix} \left[2(V_{base1} - V_{base2}) + 2V_{ref1} - 2V_{ref2} - R_{eq} I_d\right] / L_{eq} \\ -k_2 V_{ref1} \\ k_1 I_d - k_2 V_{ref2} \end{bmatrix}$	$a_2 = \begin{bmatrix} \left[2(V_{base1} - V_{base2}) + 2V_{ref1} - 2V_{ref2} - R_{eq} I_d\right] / L_{eq} \\ -k_1 I_d - k_2 V_{ref1} \\ -k_2 V_{ref2} \end{bmatrix}$
$\overline{E}_1 = \begin{bmatrix} 1 & 0 & 0 & I_d \end{bmatrix}$	$\overline{E}_2 = \begin{bmatrix} -1 & 0 & 0 & -I_d \end{bmatrix}$
$\overline{F}_1 = \begin{bmatrix} 1 & 0 & 0 & I_d \\ 0 & 0 & 0 & 0 \\ 1 & 0 & 0 & 0 \\ 0 & 0 & 0 & 0 \end{bmatrix}$	$\overline{F}_2 = \begin{bmatrix} 0 & 0 & 0 & 0 \\ -1 & 0 & 0 & -I_d \\ 1 & 0 & 0 & 0 \\ 0 & 0 & 0 & 0 \end{bmatrix}$

The reason for this lies in the construction of the $\overline{P}_i$ matrices. Recall that these matrices were defined such that

$$\overline{P}_i = \overline{F}_i^T T \overline{F}_i, \tag{5.21}$$

where T is a full symmetric matrix. As a simple example, let us take

$$\overline{F}_1 = \begin{bmatrix} 1 & 1 \\ 1 & 1 \end{bmatrix} \text{ and } T = \begin{bmatrix} a_{11} & a_{12} \\ a_{12} & a_{22} \end{bmatrix}.$$

for $i = 1$. Then,

$$\overline{P}_1 = \begin{bmatrix} (a_{11} + 2a_{12} + a_{22}) & (a_{11} + 2a_{12} + a_{22}) \\ (a_{11} + 2a_{12} + a_{22}) & (a_{11} + 2a_{12} + a_{22}) \end{bmatrix}. \tag{5.22}$$

Thus, a particular entry in $\overline{P}_1$ can take on any value depending on the entries in T, but the structure of the $\overline{P}_1$ matrix, determined by $\overline{F}_1$, is restricted such that all its entries are equal.

It turns out that it is only when the $\overline{F}_i$ matrices possess full column rank that the $\overline{P}_i$ matrices are allowed to take on any structure[2]. Otherwise, their structure is predetermined, as is the case for the system under consideration and the example shown above. Thus, even though a quadratic Lyapunov function does exist, a piecewise quadratic Lyapunov function is not found by solving the linear matrix inequalities developed in the theorem.

5.2.2 *Analysis of Dual-Cell Converter Model using UC3907*

Let us now try to apply the approach of [2] to the current-sharing scheme used in Unitrode's *UC3907* current sharing IC. As described in Chapter 2, this approach employs boundary constraints on the reference voltages. The base and saturation constraints on these voltages will produce divisions in state-space for the reference voltage state variables as well, and thus may meet the criterion of full rank $\overline{F}_i$ matrices that was not met in the previous system.

Recall the following state equations for the model of the paralleled dual-cell converter system using the *UC3907* for $i = 1,2$:

$$\frac{di_{outi}}{dt} = \frac{\Delta v_{refi} + V_{basei} - v_o - i_{outi}R}{L}, \tag{5.23a}$$

$$\frac{d\Delta v_{refi}}{dt} = k_1 \underbrace{\left[i_{\max} - i_{outi} - \Delta I\right]}_{\alpha_i}, \tag{5.23b}$$

where the state equations for the reference voltages are only valid within the base and saturation bounds. In other words,

[2] The $\overline{F}_i$ matrices for all the examples found in [2] have full column rank.

$$\frac{d\Delta v_{refi}}{dt} = \begin{cases} k_1\alpha_i, & \text{for } \Delta v_{refi} \le 0 \\ k_1\alpha_i, & \text{for } 0 \le \Delta v_{refi} \le V_{sati} \\ 0, & \text{for } \Delta v_{refi} \ge V_{sati} \end{cases} \qquad \text{for } \alpha_i > 0 \tag{5.24a}$$

$$\frac{d\Delta v_{refi}}{dt} = \begin{cases} 0, & \text{for } \Delta v_{refi} \le 0 \\ k_1\alpha_i, & \text{for } 0 \le \Delta v_{refi} \le V_{sati} \\ k_1\alpha_i, & \text{for } \Delta v_{refi} \ge V_{sati} \end{cases} \qquad \text{for } \alpha_i < 0 \tag{5.24b}$$

The analysis performed in this chapter will also be for the simplified case without load dynamics. Again, it is unnecessary to keep both output currents as our state variables. This time, however, we need to let our new state variable be $i_d = i_{out1} - i_{out2} - \Delta I$. The introduction of the ΔI term into the new state variable is necessary because the difference between i_{out1} and i_{out2} decays to ΔI, not zero if this system is stable; recall that the methods used by Johansson and Rantzer assume that the equilibrium state is at zero. The state evolution of i_d is thus given by

$$\frac{di_d}{dt} = \frac{2\left(\Delta v_{ref1} - \Delta v_{ref2}\right) + 2\left(V_{base1} - V_{base2}\right) - \left(i_d + \Delta I\right)R_{eq}}{L_{eq}}, \tag{5.25}$$

where again $L_{eq} = 2L$, and $R_{eq} = 2R$.

Keeping in mind that there are base and saturation limits on the reference voltages, the evolution of the reference voltages can be broken down subject to the value of i_d, as shown below:

- $i_d > 0 \Rightarrow i_{out1} = i_{\max}$

$$\frac{d\Delta v_{ref1}}{dt} = -k_2\Delta I < 0 \qquad \Rightarrow \Delta v_{ref1} \text{ driven downward unless at zero} \tag{5.26a}$$

$$\frac{d\Delta v_{ref2}}{dt} = k_2 i_d > 0 \qquad \Rightarrow \Delta v_{ref2} \text{ driven upward unless at saturation}$$

- $-\Delta I < i_d < -0 \Rightarrow i_{out1} = i_{\max}$

$$\frac{d\Delta v_{ref1}}{dt} = -k_2 \Delta I < 0 \quad \Rightarrow \quad \Delta v_{ref1} \text{ driven downward unless at zero} \tag{5.26b}$$

$$\frac{d\Delta v_{ref2}}{dt} = k_2 i_d < 0 \quad \Rightarrow \quad \Delta v_{ref2} \text{ driven downward unless at zero}$$

- $-2\Delta I < i_d < -\Delta I \;\Rightarrow\; i_{out2} = i_{\max}$

$$\frac{d\Delta v_{ref1}}{dt} = k_2\left(-i_d - 2\Delta I\right) < 0 \quad \Rightarrow \quad \Delta v_{ref1} \text{ driven downward unless at zero} \tag{5.26c}$$

$$\frac{d\Delta v_{ref2}}{dt} = -k_2 \Delta I < 0 \quad \Rightarrow \quad \Delta v_{ref2} \text{ driven downward unless at zero}$$

- $i_d < -2\Delta I \;\Rightarrow\; i_{out2} = i_{\max}$

$$\frac{d\Delta v_{ref1}}{dt} = k_2\left(-i_d - 2\Delta I\right) > 0 \quad \Rightarrow \quad \Delta v_{ref1} \text{ driven upward unless at saturation} \tag{5.26d}$$

$$\frac{d\Delta v_{ref2}}{dt} = -k_2 \Delta I < 0 \quad \Rightarrow \quad \Delta v_{ref2} \text{ driven downward unless at zero}$$

Thus, the possible regions for the three state variables are as shown in Table 5.2. Accounting for all possibilities, $4 \times 3 \times 3 = 36$ is the total number of piecewise affine regions that represent the nonlinear dynamics of this system. Appendix C uses state equations for i_d, Δv_{ref1} and Δv_{ref2}, as well as the boundary conditions on each region to arrive at the linear dynamics of the system in each of these 36 regions.

Finding a Lyapunov function for the system composed of these piecewise affine subsystems involves solving Linear Matrix Inequalities (LMIs) using optimization routines, as described in the theorem for piecewise quadratic stability by Johansson and Rantzer [2]. Appendix C provides the information needed to arrive at the matrices necessary to apply this theorem.

Table 5.2: State-space regions for the dual-cell converter model using *UC3907*

4 Possible Regions for i_d	3 Possible Regions for Δv_{ref1}	3 Possible Regions for Δv_{ref2}
$i_d > 0$	$\Delta v_{ref1} \leq 0$	$\Delta v_{ref2} \leq 0$
$-\Delta I < i_d < 0$	$0 < \Delta v_{ref1} < V_{sat1}$	$0 < \Delta v_{ref2} < V_{sat2}$
$-2\Delta I < i_d < -\Delta I$	$\Delta v_{ref1} \geq V_{sat1}$	$\Delta v_{ref2} \geq V_{sat2}$
$i_d < -2\Delta I$		

Even in the simple case of two converters in parallel with no load dynamics, the number of variables in our LMI system is extremely large. The T matrix is size 10×10, and each of the 36 U_i and W_i matrices is 7×7. The problem arises when we realize that each coefficient in the matrices U_i and W_i is required to be non-negative, and thus, in accordance with available LMI software, must be considered an LMI variable. Keeping in mind that these matrices are all symmetric, the number of LMI variables in our setup is a little under 1800! This is extremely large, considering not only the simplicity of our system, but also the lack of software available to handle an LMI problem of this magnitude. The `LMI Control Toolbox` in `MATLAB` is designed to handle up to 1000 variables, and other available LMI tools can only handle a similar number of variables.

5.3 Summary

As seen in the previous sections, the structure of the theorem introduced by Johansson and Rantzer [2], although mathematically attractive, has certain limitations. First, the structure of the $\overline{P}_i$ matrices is determined by the structure of the $\overline{F}_i$ matrices, which is fixed in turn by the boundary conditions arising from the divisions in state-space. Even if the $\overline{P}_i$ matrices have full rank, however, a simple system analyzed by this theorem can produce a large number of variables beyond the capabilities of available software. Also, the implementation of the LMI software in `MATLAB` does not allow the U_i and W_i matrices to have zero entries, unless forced by the user. Thus, if $\overline{P}_i$ matrices could be found by allowing some entries of these matrices to be zero, the software will not find them, unless the user has prior information and forces these entries to zero. These factors, introduced by both the theorem and available software, severely limit the types of systems that can be successfully analyzed through the method presented in [2].

6 Concluding Remarks

This thesis explored several avenues to assess the stability of open- or closed-loop symmetrically-coupled nonlinear systems. For systems with large numbers of coupled subsystems, it is first desirable to reduce the order of the system to make analysis and control tractable. Lunze used linear transformations to reduce the stability analysis of a linear open-loop symmetric system consisting of N subsystems to that of a model of order twice that of the subsystem order [1]. We first extended Lunze's analysis to feedback systems, and then further extended it to include nonlinear couplings.

The similarity transformation used to dissect nonlinear systems of this type is successful not only in transforming the system into reduced order differential- and common-mode configurations, but also in confining the nonlinearity present to the common-mode configuration of the transformed system. Furthermore, there were no state-variables that were fed back from the common to the differential-mode circuits, and thus the stability of the reduced-order nonlinear system was easy to establish. The stability of these reduced-order subsystems was then used to guarantee stability of the overall system. It was determined that this analysis could be applied to a wide variety of nonlinear couplings that met certain constraints.

As an example, we analyzed a paralleled current-mode-controlled converter system using the same similarity transformation. A three-cell system was first analyzed and simulated, and the results for this paralleled converter system were then generalized to the N-cell case. As expected, the original nonlinear system is transformed into differential- and common-mode subsystems. The nonlinearity is restricted once again to the common-mode configuration, as is the load. Circuit-based analysis was used to gauge stability of this system; for stability analysis, it is only necessary to assess the stability of one of the (identical) differential-mode circuits, along with the common-mode circuit. The differential-mode circuits are linear, and the nonlinearity of the system is simply captured in the current source of the common-mode circuit. A candidate Lyapunov function, based upon the energy in the active elements in the common- and

differential-mode configurations, is also found to guarantee the stability of this *N*-cell paralleled current-mode-controlled converter system.

Because some symmetrically-coupled systems with nonlinear feedback can be modeled as hybrid systems, tools developed to examine such systems were also examined. Johansson and Rantzer [2] proposed partitioning the state-space of a nonlinear system with piecewise affine dynamics into a number of closed cells, and then searching for a piecewise continuous Lyapunov function to guarantee the stability of the overall system, using methods from the Linear Matrix Inequality (LMI) framework. This proposed method was used to analyze a specific system involving paralleled current-mode-controlled power converters. The control systems used for demonstration purposes were based on each converter comparing its own current to the maximum of all currents. The analysis of this example brought to light some constraints and limitations of the theorem in [2] and of available LMI software.

A Verification of Lyapunov Function

Lunze reduces the stability analysis of the nNth-order matrix $\tilde{A}$ that governs a symmetric system to that of two nth-order matrices A_d and A_c [1]. If we have Lyapunov functions for both A_d and A_c, what will be the Lyapunov function for the overall system? In order to arrive at this answer, we must work back through the similarity transformation T.

Let's assume that the two matrices, A_d and A_c, are stable. Then Lyapunov functions for the system described by these matrices exist, and are defined by

$$V_{di} = \tilde{x}_i^T P_d \tilde{x}_i \qquad \text{for } i = 1,2,..,(N-1), \tag{A.1a}$$

$$V_c = \tilde{x}_N^T P_c \tilde{x}_N \tag{A.1b}$$

where

$$A_d^T P_d + P_d A_d = -Q_d \quad \text{for } Q_d \geq 0, \tag{A.2a}$$

$$A_c^T P_c + P_c A_c = -Q_c \quad \text{for } Q_c \geq 0. \tag{A.2b}$$

Thus, the Lyapunov function $\tilde{V}$ of the transformed system is given by

$$\tilde{V} = \tilde{x}^T \underbrace{\left[\begin{array}{cccc|c} P_d & 0 & \cdots & 0 & 0 \\ 0 & P_d & \cdots & 0 & 0 \\ \vdots & \vdots & & \vdots & \vdots \\ 0 & 0 & \cdots & P_d & 0 \\ \hline 0 & 0 & \cdots & 0 & P_c \end{array}\right]}_{\tilde{P}} \tilde{x} \; . \tag{A.3}$$

Note that when simplified

$$\tilde{V} = \sum_{i=1}^{N-1} \tilde{x}_i^T P_d \tilde{x}_i + \tilde{x}_N^T P_c \tilde{x}_N = \sum_{i=1}^{N-1} V_{di} + V_c . \tag{A.4}$$

This Lyapunov function for the transformed system can be rewritten as a function of the variables x_1 through x_N to arrive at the Lyapunov function for the original dual-cell converter system.

B LMI Software

The Piecewise Linear Toolbox (PWL), obtained from M. Johansson at the Lund Institute of Technology, interfaces to the LMI Control Toolbox in MATLAB. This toolbox was designed to handle P_i matrices of size 2×2 or 3×3 only. Furthermore, it was designed to fix the structure of matrices U_i and W_i by forcing their diagonal entries to zero; this was not only sufficient for the examples used by Johansson and Rantzer [2,3], but perhaps also necessary. Recall that the piecewise quadratic stability theorem requires non-negative entries in these matrices. The LMI Control Toolbox, however, allows these entries to be defined as LMI variables that are restricted to being positive, but not zero. Thus, if a Lyapunov function can be found only if some of the coefficients in U_i and W_i are zero, the software will fail in finding one because the LMI software being used will not consider this case.

The PWL toolbox was thus modified to handle the problems we wished to address. The modified toolbox is capable of handling P_i matrices of any reasonable size. The U_i and W_i matrices in our system do not necessary have zero entries on their diagonals, and thus they were redefined as full symmetric matrices. As stated earlier, this does not allow any zero entries.

Both the original and the modified versions of the PWL toolbox require that the $\tilde{A}_i$, $\tilde{E}_i$, and $\tilde{F}_i$ matrices be defined such that their dimensions are compatible, as dictated by the piecewise quadratic stability theorem.

B.1 Modified Toolbox Files

Two files were modified to accommodate the changes mentioned above. They are included below. In the first file, *addynamics.m*, a couple lines of code were added as indicated. The second file, *lyap.m*, is a revision of the original file *pqstab.m*.

B.1.1 Addynamics.m

```
% dyn = addynamics(A, a, B, C, c, D)
%
% Adds a new dynamics specification to the
% piecewise linear system currently described.
% A label can be optionally attached to this
% specification to facilitate future reference to it.
%
% Input:
%     A, a, B,
%     C, c, D
%     Data describing the dynamics
%
% Output:
%     DYN         A label for future reference to the dynamics
%

function dyn = addynamics(A, a, B, C, c, D)

global GLF_REG GLF_DYN GLF_NREG GLF_NDYN GLF_N

ni = nargin;

% Added Code
global NO_a
if (ni<2)
      NO_a = 1;
else
      NO_a = isempty(a);
end
% End of Added Code

if (ni < 1) | (ni > 6)
      error('Wrong number of function input arguments');
end

n = size(A,1);
if GLF_NDYN == 0
      GLF_N = n;
end

NoInp  = 1;
NoOutp = 1;

if ni >= 3
      if ~(isempty(B))
            NoInp = size(B,2);
      end
end

if ni >= 4
      NoOutp = size(C,1);
end
```

```
if ni < 6
      D = zeros(NoOutp, NoInp);
      if ni < 5
            c = zeros(NoOutp, 1);
            if ni < 4
                  C = zeros(NoOutp, n);
                  if ni < 3
                        B = zeros(n, NoInp);
                        if ni < 2
                              a = zeros(n, 1);
                        end
                  end
            end
      end
end

if isempty(a)
      a = zeros(n,1);
end

if isempty(B)
      B = zeros(n, NoInp);
end

if isempty(C)
      C = zeros(NoOutp, n);
end

if isempty(c)
      c = zeros(NoOutp, 1);
end

if isempty(D)
      D = zeros(NoOutp, NoInp);
end

global GLF_REG GLF_DYN GLF_NREG GLF_NDYN

if (isempty(GLF_NDYN))
      error('Use SETPWL to initialize the piecewise linear system');
end

GLF_NDYN = GLF_NDYN + 1;
GLF_DYN(GLF_NDYN).a = a;
GLF_DYN(GLF_NDYN).A = A;
GLF_DYN(GLF_NDYN).B = B;
GLF_DYN(GLF_NDYN).C = C;
GLF_DYN(GLF_NDYN).D = D;
GLF_DYN(GLF_NDYN).c = c;
dyn = GLF_NDYN;
```

B.1.2 Lyap.m

```
% [P, NoLMIs, NoVars] = lyap(pwlsys, options)
%
% MODIFIED COPY OF PQSTAB.M
%
% Search for a piecewise quadratic Lyapunov function to verify
% stability of a piecewise linear system.
%
% Input:
%    PWLSYS    Piecewise linear system.
%    OPTIONS   Options used by LMI-Lab.
%
% Output:
%    P     If there exist a piecewise quadratic Lyapunov function, V,
%          then P is a n-dimensional array arranged such that
%          [x; 1]'*P(:,:,i)*[x; 1] describes the Lyapunov function
%          corresponding to region number i. If no piecewise
%          quadratic Lyapunov function exist, the function will
%          return an empty array, P = [].
%  NoLMIs  Number of LMIs needed to solve the problem
%  NoVars  Number of decision variables needed for the LMIs
%

function [P, NoLMIs, NoVars] = lyap(pwl, options)

% Added variable
global NO_a

ni = nargin;
if ni == 1
     options = [];
end;

NoE  = size(pwl.Region,2);
dimn = size(pwl.Dynamics(1).A, 1);
dimf = size(pwl.Region(1).F, 1);

setlmis([]);

[Tt,n,Ttdec] = lmivar(1,[dimf 1]);          % lmivar T

ltcount = 0;
UWcnt    = 0;

for lp = 1:NoE
     co = pwl.Region(lp).co;
     Ei = pwl.Region(lp).E;

     Fi = pwl.Region(lp).F;
     Idx = pwl.Region(lp).Idx;
     dimp = size(Ei, 1);

     for lp4 = 1:length(Idx)
          UWcnt = UWcnt + 1;
          Ai = pwl.Dynamics(Idx(lp4)).A;
```

```
        if (~NO_a)  % Added => Originally = if(~co)
              ai = pwl.Dynamics(Idx(lp4)).a;
              Ai = [Ai, ai; zeros(1, dimn+1)];
        end
        U = zeros(dimp);
        W = zeros(dimp);
        for lp2 = 1:dimp-1
              for lp3 = 1:(dimp-lp2)
                    [tmpU, n, U(dimp+1-lp2,lp3)] = lmivar(1,[1 1]);
                    % lmivar Uijk

                    ltcount = ltcount + 1;      % force Uijk > 0
                    lmiterm([-ltcount 1 1 tmpU],1,1);

                    [tmpW, n, W(dimp+1-lp2,lp3)] = lmivar(1,[1 1]);
                    %lmivar Wijk

                    ltcount = ltcount + 1;      % force Wijk > 0
                    lmiterm([-ltcount 1 1 tmpW],1,1);
              end
        end

        % Added to allow the diagonals of U,W matrices be nonzero
        UWdiag = 1;
        U1 = U;
        W1 = W;
        if(UWdiag)
              for lp5 = 1: dimp
                    [tmpU, n, U(lp5,lp5)] = lmivar(1,[1 1]);
                    ltcount = ltcount + 1;
                    lmiterm([-ltcount 1 1 tmpU],1,1);
                    [tmpW, n, W(lp5,lp5)] = lmivar(1,[1 1]);
                    ltcount = ltcount + 1;
                    lmiterm([-ltcount 1 1 tmpW],1,1);
              end
        end

        lv(UWcnt).U = lmivar(3, U+U1');
        lv(UWcnt).W = lmivar(3, W+W1');

        ltcount = ltcount + 1;            % 0 > Ai'Pi+PiAi+Ei'UiEi

        lmiterm([ltcount 1 1 Tt],Fi',Fi*Ai,'s');

        if ~isempty(lv(UWcnt).U)
              lmiterm([ltcount 1 1 lv(UWcnt).U],Ei',Ei);
        end

        ltcount = ltcount + 1;            % 0 < Pi-Ei'WiEi
        lmiterm([-ltcount 1 1 Tt],Fi',Fi);
        if ~isempty(lv(UWcnt).W)
              lmiterm([ltcount 1 1 lv(UWcnt).W],Ei',Ei);
        end
    end
end
```

```
lmisyst = getlmis;
NoLMIs  = ltcount;
NoVars  = decnbr(lmisyst);

[tmin,lmisystfeas] = feasp(lmisyst, options);
if (tmin < 0)
     T = dec2mat(lmisyst, lmisystfeas, Tt);

     if ~isempty(lv(UWcnt).U)
          U = dec2mat(lmisyst, lmisystfeas, lv(UWcnt).U);
     end

     if ~isempty(lv(UWcnt).W)
          W = dec2mat(lmisyst, lmisystfeas, lv(UWcnt).W);
     end

     dimP = size(pwl.Region(1).F,2);
     P = zeros(dimP,dimP,NoE);

     for lp = 1:NoE
          Fi = pwl.Region(lp).F;
          tdi = size(Fi,2);
          P(1:tdi,1:tdi,lp) = Fi'*T*Fi;
     end

else
     P = [];
end
```

B.2 Sample Code *NoLoad.m*

```
% PWL Toolbox Code
% This is the system with two converters with no load dynamics.
% Both base & saturation constraints on vrefi's have been eliminated.
% Also Delta I on id has been eliminated.
%
% Offsets Vo1 & Vo2 have been added to each vrefi.
% There are only two regions now => id > 0 and id < 0.
% Our state variables, however, are now the perturbed variables =>
% id = Id + id_tild where id_tild is one of our new state variables.
% vref1_tild and vref2_tild are the other two.

function noload;

% Constants...
k1 = 5;
k2 = 10;
Req = 2;
Leq = 0.1;

% Vo1 > Vo2 for the Operating Point to be Valid
Vo1 = 0.01;
```

```
Vo2 = 0;
Vodiff = Vo1-Vo2;

optns = [0 0 0 0 1];

% Computing Operating Point...
VREF1 = 0;
VREF2 = (2*k1*Vodiff)/(2*k1 + Req*k2);
ID = 2*(VREF2*k2)/(2*k1);

% Dynamics & Trajectories
% Region I =>  id > 0   OR   id_tild > -ID;
% Region II => id < 0   OR   id_tild < -ID;
A1 = [-Req/Leq 2/Leq -2/Leq; 0 -k2 0; k1 0 -k2];
A2 = [-Req/Leq 2/Leq -2/Leq; -k1 -k2 0; 0 0 -k2];

a = zeros(3,2);
for i=1:2,
     a(1,i) = 2*[Vodiff + VREF1 - VREF2 - (Req*ID/2)]/Leq;
     a(2,i) = -k1*ID*(i==2) - k2*VREF1;
     a(3,i) = k1*ID*(i==1) - k2*VREF2;
end

E1 = [1 0 0 ID];
E2 = [-1 0 0 -ID];

F1 = [1 0 0 ID;
     0 0 0 0;
     1 0 0 0;
     0 0 0 0];

F2 = [0 0 0 0;
     -1 0 0 -ID;
     1 0 0 0;
     0 0 0 0];

% Initialize & Setup System
setpwl([]);

dyn1 = addynamics(A1,a(:,1));
dyn2 = addynamics(A2,a(:,2));

addregion(E1, F1, dyn1);
addregion(E2, F2, dyn2);

pwlsyst = getpwl;

% Simulate System
disp('Simulating the system...');
[t, xv, te, region] = pwlsim(pwlsyst, [0 0.01 -0.01]', [0 10]);
disp('Done!');

% Compute Global Lyapunov Function
disp('Computing global quadratic Lyapunov function...')
P = qstab(pwlsyst, optns);
```

```
if ~isempty(P)
      P = P
      eigen_P = zeros(3,1);
      eigen_P = eig(P)

      % Plot Lyapunov function
      V = zeros(size(t));
      for i=1:size(t),
      vec = [xv(i,1) xv(i,2) xv(i,3)]';
      V(i) = vec'*P*vec;
      eplot(t,xv(:,1),xv(:,2),xv(:,3),V,2);

else
      disp('Unable to find one!');

      % Computer Piecewise Lyapunov Function
      disp('Computing piecewise quadratic Lyapunov function...');
      [P, NoL, NoV] = lyap(pwlsyst, optns);

      if ~isempty(P)
            fprintf('Solution found using %d LMIs and %d
                  variables.\n\n',NoL,NoV);
      else
            disp('Unable to find one!');
      end
end
```

C Divisions of State-Space of the Dual-Cell Paralleled Power Converter Model

The tables listed in the following pages of this appendix segment the non-linear dynamics of the dual-cell paralleled power converter model using *UC3907* in the absence of load dynamics into 36 linear state-space regions. Each region is represented by $X_{\alpha\beta\gamma}$, closed subsets of $\Re^3$. The subscript α represents the state of i_d, β represents the state of Δv_{ref1} and γ represents the state of Δv_{ref2}.

In these tables

$$\underbrace{\begin{bmatrix} \dot{i}_d \\ \Delta\dot{v}_{ref1} \\ \Delta\dot{v}_{ref2} \end{bmatrix}}_{\dot{x}} = A_{\alpha\beta\gamma} \cdot \underbrace{\begin{bmatrix} i_d \\ \Delta v_{ref1} \\ \Delta v_{ref2} \end{bmatrix}}_{x} + B_{\alpha\beta\gamma} \tag{C.1}$$

and $V_{basediff} = V_{base1} - V_{base2}$.

Matrices for use in the theorem by Johansson and Rantzer are defined as follows:

$$\overline{A}_i = \begin{bmatrix} A_i & B_i \\ 0 & 0 \end{bmatrix}, \ \overline{E}_i = \begin{bmatrix} C_i & D_i \end{bmatrix}, \text{ and } \overline{F}_i = \begin{bmatrix} C_i & D_i \\ I & 0 \end{bmatrix} \tag{C.2}$$

Table C.1: $A_{\alpha\beta\gamma}$ and $B_{\alpha\beta\gamma}$ for Regions where $i_d > 0$.

	$\Delta v_{ref1} \le 0$	$0 < \Delta v_{ref1} < V_{sat1}$	$\Delta v_{ref1} \ge V_{sat1}$
$\Delta v_{ref2} \le 0$	$A_{111} = \begin{bmatrix} \frac{-R_{eq}}{L_{eq}} & \frac{2}{L_{eq}} & \frac{-2}{L_{eq}} \\ 0 & 0 & 0 \\ k_1 & 0 & 0 \end{bmatrix}$, $B_{111} = \begin{bmatrix} \frac{2V_{basediff} - R_{eq}\Delta I}{L_{eq}} \\ 0 \\ 0 \end{bmatrix}$	$A_{121} = \begin{bmatrix} \frac{-R_{eq}}{L_{eq}} & \frac{2}{L_{eq}} & \frac{-2}{L_{eq}} \\ 0 & 0 & 0 \\ k_1 & 0 & 0 \end{bmatrix}$, $B_{121} = \begin{bmatrix} \frac{2V_{basediff} - R_{eq}\Delta I}{L_{eq}} \\ -k_1\Delta I \\ 0 \end{bmatrix}$	$A_{131} = \begin{bmatrix} \frac{-R_{eq}}{L_{eq}} & \frac{2}{L_{eq}} & \frac{-2}{L_{eq}} \\ 0 & 0 & 0 \\ k_1 & 0 & 0 \end{bmatrix}$, $B_{131} = \begin{bmatrix} \frac{2V_{basediff} - R_{eq}\Delta I}{L_{eq}} \\ -k_1\Delta I \\ 0 \end{bmatrix}$
$0 < \Delta v_{ref2} < V_{sat2}$	$A_{112} = \begin{bmatrix} \frac{-R_{eq}}{L_{eq}} & \frac{2}{L_{eq}} & \frac{-2}{L_{eq}} \\ 0 & 0 & 0 \\ k_1 & 0 & 0 \end{bmatrix}$, $B_{112} = \begin{bmatrix} \frac{2V_{basediff} - R_{eq}\Delta I}{L_{eq}} \\ 0 \\ 0 \end{bmatrix}$	$A_{122} = \begin{bmatrix} \frac{-R_{eq}}{L_{eq}} & \frac{2}{L_{eq}} & \frac{-2}{L_{eq}} \\ 0 & 0 & 0 \\ k_1 & 0 & 0 \end{bmatrix}$, $B_{122} = \begin{bmatrix} \frac{2V_{basediff} - R_{eq}\Delta I}{L_{eq}} \\ -k_1\Delta I \\ 0 \end{bmatrix}$	$A_{132} = \begin{bmatrix} \frac{-R_{eq}}{L_{eq}} & \frac{2}{L_{eq}} & \frac{-2}{L_{eq}} \\ 0 & 0 & 0 \\ k_1 & 0 & 0 \end{bmatrix}$, $B_{132} = \begin{bmatrix} \frac{2V_{basediff} - R_{eq}\Delta I}{L_{eq}} \\ -k_1\Delta I \\ 0 \end{bmatrix}$
$\Delta v_{ref2} \ge V_{sat2}$	$A_{113} = \begin{bmatrix} \frac{-R_{eq}}{L_{eq}} & \frac{2}{L_{eq}} & \frac{-2}{L_{eq}} \\ 0 & 0 & 0 \\ 0 & 0 & 0 \end{bmatrix}$, $B_{113} = \begin{bmatrix} \frac{2V_{basediff} - R_{eq}\Delta I}{L_{eq}} \\ 0 \\ 0 \end{bmatrix}$	$A_{123} = \begin{bmatrix} \frac{-R_{eq}}{L_{eq}} & \frac{2}{L_{eq}} & \frac{-2}{L_{eq}} \\ 0 & 0 & 0 \\ 0 & 0 & 0 \end{bmatrix}$, $B_{123} = \begin{bmatrix} \frac{2V_{basediff} - R_{eq}\Delta I}{L_{eq}} \\ -k_1\Delta I \\ 0 \end{bmatrix}$	$A_{133} = \begin{bmatrix} \frac{-R_{eq}}{L_{eq}} & \frac{2}{L_{eq}} & \frac{-2}{L_{eq}} \\ 0 & 0 & 0 \\ 0 & 0 & 0 \end{bmatrix}$, $B_{133} = \begin{bmatrix} \frac{2V_{basediff} - R_{eq}\Delta I}{L_{eq}} \\ -k_1\Delta I \\ 0 \end{bmatrix}$

Table C.2: $C_{\alpha\beta\gamma}$ and $D_{\alpha\beta\gamma}$ for Regions where $i_d > 0$.

	$\Delta v_{ref1} \le 0$	$0 < \Delta v_{ref1} < V_{sat1}$	$\Delta v_{ref1} \ge V_{sat1}$
$\Delta v_{ref2} \le 0$	$C_{111} = \begin{bmatrix} 1 & 0 & 0 \\ 0 & 0 & 0 \\ 0 & 0 & 0 \\ 0 & -1 & 0 \\ 0 & 0 & 0 \\ 0 & 0 & -1 \end{bmatrix}$, $D_{111} = \begin{bmatrix} 0 \\ 0 \\ 0 \\ 0 \\ 0 \\ 0 \end{bmatrix}$	$C_{121} = \begin{bmatrix} 1 & 0 & 0 \\ 0 & 0 & 0 \\ 0 & 1 & 0 \\ 0 & -1 & 0 \\ 0 & 0 & 0 \\ 0 & 0 & -1 \end{bmatrix}$, $D_{121} = \begin{bmatrix} 0 \\ 0 \\ 0 \\ V_{sat1} \\ 0 \\ 0 \end{bmatrix}$	$C_{131} = \begin{bmatrix} 1 & 0 & 0 \\ 0 & 0 & 0 \\ 0 & 1 & 0 \\ 0 & 0 & 0 \\ 0 & 0 & 0 \\ 0 & 0 & -1 \end{bmatrix}$, $D_{131} = \begin{bmatrix} 0 \\ 0 \\ -V_{sat1} \\ 0 \\ 0 \\ 0 \end{bmatrix}$
$0 < \Delta v_{ref2} < V_{sat2}$	$C_{112} = \begin{bmatrix} 1 & 0 & 0 \\ 0 & 0 & 0 \\ 0 & 0 & 0 \\ 0 & -1 & 0 \\ 0 & 0 & 1 \\ 0 & 0 & -1 \end{bmatrix}$, $D_{112} = \begin{bmatrix} 0 \\ 0 \\ 0 \\ 0 \\ 0 \\ V_{sat2} \end{bmatrix}$	$C_{122} = \begin{bmatrix} 1 & 0 & 0 \\ 0 & 0 & 0 \\ 0 & 1 & 0 \\ 0 & -1 & 0 \\ 0 & 0 & 1 \\ 0 & 0 & -1 \end{bmatrix}$, $D_{122} = \begin{bmatrix} 0 \\ 0 \\ 0 \\ V_{sat1} \\ 0 \\ V_{sat2} \end{bmatrix}$	$C_{132} = \begin{bmatrix} 1 & 0 & 0 \\ 0 & 0 & 0 \\ 0 & 1 & 0 \\ 0 & 0 & 0 \\ 0 & 0 & 1 \\ 0 & 0 & -1 \end{bmatrix}$, $D_{132} = \begin{bmatrix} 0 \\ 0 \\ -V_{sat1} \\ 0 \\ 0 \\ V_{sat2} \end{bmatrix}$
$\Delta v_{ref2} \ge V_{sat2}$	$C_{113} = \begin{bmatrix} 1 & 0 & 0 \\ 0 & 0 & 0 \\ 0 & 0 & 0 \\ 0 & -1 & 0 \\ 0 & 0 & 1 \\ 0 & 0 & 0 \end{bmatrix}$, $D_{113} = \begin{bmatrix} 0 \\ 0 \\ 0 \\ 0 \\ -V_{sat2} \\ 0 \end{bmatrix}$	$C_{123} = \begin{bmatrix} 1 & 0 & 0 \\ 0 & 0 & 0 \\ 0 & 1 & 0 \\ 0 & -1 & 0 \\ 0 & 0 & 1 \\ 0 & 0 & 0 \end{bmatrix}$, $D_{123} = \begin{bmatrix} 0 \\ 0 \\ 0 \\ V_{sat1} \\ -V_{sat2} \\ 0 \end{bmatrix}$	$C_{133} = \begin{bmatrix} 1 & 0 & 0 \\ 0 & 0 & 0 \\ 0 & 1 & 0 \\ 0 & 0 & 0 \\ 0 & 0 & 1 \\ 0 & 0 & 0 \end{bmatrix}$, $D_{133} = \begin{bmatrix} 0 \\ 0 \\ -V_{sat1} \\ 0 \\ -V_{sat2} \\ 0 \end{bmatrix}$

Table C.3: $A_{\alpha\beta\gamma}$ and $B_{\alpha\beta\gamma}$ for Regions where $(-\Delta I) < i_d < 0$.

	$\Delta v_{ref1} \le 0$	$0 < \Delta v_{ref1} < V_{sat1}$	$\Delta v_{ref1} \ge V_{sat1}$
$\Delta v_{ref2} \le 0$	$A_{211} = \begin{bmatrix} \frac{-R_{eq}}{L_{eq}} & \frac{2}{L_{eq}} & \frac{-2}{L_{eq}} \\ 0 & 0 & 0 \\ 0 & 0 & 0 \end{bmatrix}$, $B_{211} = \begin{bmatrix} \frac{2V_{basediff} - R_{eq}\Delta I}{L_{eq}} \\ 0 \\ 0 \end{bmatrix}$	$A_{221} = \begin{bmatrix} \frac{-R_{eq}}{L_{eq}} & \frac{2}{L_{eq}} & \frac{-2}{L_{eq}} \\ 0 & 0 & 0 \\ 0 & 0 & 0 \end{bmatrix}$, $B_{221} = \begin{bmatrix} \frac{2V_{basediff} - R_{eq}\Delta I}{L_{eq}} \\ -k_1\Delta I \\ 0 \end{bmatrix}$	$A_{231} = \begin{bmatrix} \frac{-R_{eq}}{L_{eq}} & \frac{2}{L_{eq}} & \frac{-2}{L_{eq}} \\ 0 & 0 & 0 \\ 0 & 0 & 0 \end{bmatrix}$, $B_{231} = \begin{bmatrix} \frac{2V_{baseduff} - R_{eq}\Delta I}{L_{eq}} \\ -k_1\Delta I \\ 0 \end{bmatrix}$
$0 < \Delta v_{ref2} < V_{sat2}$	$A_{212} = \begin{bmatrix} \frac{-R_{eq}}{L_{eq}} & \frac{2}{L_{eq}} & \frac{-2}{L_{eq}} \\ 0 & 0 & 0 \\ k_1 & 0 & 0 \end{bmatrix}$, $B_{212} = \begin{bmatrix} \frac{2V_{basediff} - R_{eq}\Delta I}{L_{eq}} \\ 0 \\ 0 \end{bmatrix}$	$A_{221} = \begin{bmatrix} \frac{-R_{eq}}{L_{eq}} & \frac{2}{L_{eq}} & \frac{-2}{L_{eq}} \\ 0 & 0 & 0 \\ k_1 & 0 & 0 \end{bmatrix}$, $B_{221} = \begin{bmatrix} \frac{2V_{basediff} - R_{eq}\Delta I}{L_{eq}} \\ -k_1\Delta I \\ 0 \end{bmatrix}$	$A_{232} = \begin{bmatrix} \frac{-R_{eq}}{L_{eq}} & \frac{2}{L_{eq}} & \frac{-2}{L_{eq}} \\ 0 & 0 & 0 \\ k_1 & 0 & 0 \end{bmatrix}$, $B_{232} = \begin{bmatrix} \frac{2V_{basediff} - R_{eq}\Delta I}{L_{eq}} \\ -k_1\Delta I \\ 0 \end{bmatrix}$
$\Delta v_{ref2} \ge V_{sat2}$	$A_{213} = \begin{bmatrix} \frac{-R_{eq}}{L_{eq}} & \frac{2}{L_{eq}} & \frac{-2}{L_{eq}} \\ 0 & 0 & 0 \\ k_1 & 0 & 0 \end{bmatrix}$, $B_{213} = \begin{bmatrix} \frac{2V_{basediff} - R_{eq}\Delta I}{L_{eq}} \\ 0 \\ 0 \end{bmatrix}$	$A_{223} = \begin{bmatrix} \frac{-R_{eq}}{L_{eq}} & \frac{2}{L_{eq}} & \frac{-2}{L_{eq}} \\ 0 & 0 & 0 \\ k_1 & 0 & 0 \end{bmatrix}$, $B_{223} = \begin{bmatrix} \frac{2V_{basediff} - R_{eq}\Delta I}{L_{eq}} \\ -k_1\Delta I \\ 0 \end{bmatrix}$	$A_{233} = \begin{bmatrix} \frac{-R_{eq}}{L_{eq}} & \frac{2}{L_{eq}} & \frac{-2}{L_{eq}} \\ 0 & 0 & 0 \\ k_1 & 0 & 0 \end{bmatrix}$, $B_{233} = \begin{bmatrix} \frac{2V_{basediff} - R_{eq}\Delta I}{L_{eq}} \\ -k_1\Delta I \\ 0 \end{bmatrix}$

Table C.4: $C_{\alpha\beta\gamma}$ and $D_{\alpha\beta\gamma}$ for Regions where $(-\Delta I) < i_d < 0$.

	$\Delta v_{ref1} \le 0$	$0 < \Delta v_{ref1} < V_{sat1}$	$\Delta v_{ref1} \ge V_{sat1}$
$\Delta v_{ref2} \le 0$	$C_{211} = \begin{bmatrix} 1 & 0 & 0 \\ -1 & 0 & 0 \\ 0 & 0 & 0 \\ 0 & -1 & 0 \\ 0 & 0 & 0 \\ 0 & 0 & -1 \end{bmatrix}$, $D_{211} = \begin{bmatrix} \Delta I \\ 0 \\ 0 \\ 0 \\ 0 \\ 0 \end{bmatrix}$	$C_{221} = \begin{bmatrix} 1 & 0 & 0 \\ -1 & 0 & 0 \\ 0 & 1 & 0 \\ 0 & -1 & 0 \\ 0 & 0 & 0 \\ 0 & 0 & -1 \end{bmatrix}$, $D_{221} = \begin{bmatrix} \Delta I \\ 0 \\ 0 \\ V_{sat1} \\ 0 \\ 0 \end{bmatrix}$	$C_{231} = \begin{bmatrix} 1 & 0 & 0 \\ -1 & 0 & 0 \\ 0 & 1 & 0 \\ 0 & 0 & 0 \\ 0 & 0 & 0 \\ 0 & 0 & -1 \end{bmatrix}$, $D_{231} = \begin{bmatrix} \Delta I \\ 0 \\ -V_{sat1} \\ 0 \\ 0 \\ 0 \end{bmatrix}$
$0 < \Delta v_{ref2} < V_{sat2}$	$C_{212} = \begin{bmatrix} 1 & 0 & 0 \\ -1 & 0 & 0 \\ 0 & 0 & 0 \\ 0 & -1 & 0 \\ 0 & 0 & 1 \\ 0 & 0 & -1 \end{bmatrix}$, $D_{212} = \begin{bmatrix} \Delta I \\ 0 \\ 0 \\ 0 \\ 0 \\ V_{sat2} \end{bmatrix}$	$C_{222} = \begin{bmatrix} 1 & 0 & 0 \\ -1 & 0 & 0 \\ 0 & 1 & 0 \\ 0 & -1 & 0 \\ 0 & 0 & 1 \\ 0 & 0 & -1 \end{bmatrix}$, $D_{222} = \begin{bmatrix} \Delta I \\ 0 \\ 0 \\ V_{sat1} \\ 0 \\ V_{sat2} \end{bmatrix}$	$C_{232} = \begin{bmatrix} 1 & 0 & 0 \\ -1 & 0 & 0 \\ 0 & 1 & 0 \\ 0 & 0 & 0 \\ 0 & 0 & 1 \\ 0 & 0 & -1 \end{bmatrix}$, $D_{232} = \begin{bmatrix} \Delta I \\ 0 \\ -V_{sat1} \\ 0 \\ 0 \\ V_{sat2} \end{bmatrix}$
$\Delta v_{ref2} \ge V_{sat2}$	$C_{213} = \begin{bmatrix} 1 & 0 & 0 \\ -1 & 0 & 0 \\ 0 & 0 & 0 \\ 0 & -1 & 0 \\ 0 & 0 & 1 \\ 0 & 0 & 0 \end{bmatrix}$, $D_{213} = \begin{bmatrix} \Delta I \\ 0 \\ 0 \\ 0 \\ -V_{sat2} \\ 0 \end{bmatrix}$	$C_{223} = \begin{bmatrix} 1 & 0 & 0 \\ -1 & 0 & 0 \\ 0 & 1 & 0 \\ 0 & -1 & 0 \\ 0 & 0 & 1 \\ 0 & 0 & 0 \end{bmatrix}$, $D_{223} = \begin{bmatrix} \Delta I \\ 0 \\ 0 \\ V_{sat1} \\ -V_{sat2} \\ 0 \end{bmatrix}$	$C_{233} = \begin{bmatrix} 1 & 0 & 0 \\ -1 & 0 & 0 \\ 0 & 1 & 0 \\ 0 & 0 & 0 \\ 0 & 0 & 1 \\ 0 & 0 & 0 \end{bmatrix}$, $D_{233} = \begin{bmatrix} \Delta I \\ 0 \\ -V_{sat1} \\ 0 \\ -V_{sat2} \\ 0 \end{bmatrix}$

Table C.5: $A_{\alpha\beta\gamma}$ and $B_{\alpha\beta\gamma}$ for Regions where $(-2\Delta I) < i_d < -\Delta I$.

	$\Delta v_{ref1} \le 0$	$0 < \Delta v_{ref1} < V_{sat1}$	$\Delta v_{ref1} \ge V_{sat1}$
$\Delta v_{ref2} \le 0$	$A_{311} = \begin{bmatrix} \frac{-R_{eq}}{L_{eq}} & \frac{2}{L_{eq}} & \frac{-2}{L_{eq}} \\ 0 & 0 & 0 \\ 0 & 0 & 0 \end{bmatrix}$, $B_{311} = \begin{bmatrix} \frac{2V_{basediff} - R_{eq}\Delta I}{L_{eq}} \\ 0 \\ 0 \end{bmatrix}$	$A_{321} = \begin{bmatrix} \frac{-R_{eq}}{L_{eq}} & \frac{2}{L_{eq}} & \frac{-2}{L_{eq}} \\ -k_1 & 0 & 0 \\ 0 & 0 & 0 \end{bmatrix}$, $B_{321} = \begin{bmatrix} \frac{2V_{basediff} - R_{eq}\Delta I}{L_{eq}} \\ -2k_1\Delta I \\ 0 \end{bmatrix}$	$A_{331} = \begin{bmatrix} \frac{-R_{eq}}{L_{eq}} & \frac{2}{L_{eq}} & \frac{-2}{L_{eq}} \\ -k_1 & 0 & 0 \\ 0 & 0 & 0 \end{bmatrix}$, $B_{331} = \begin{bmatrix} \frac{2V_{basediff} - R_{eq}\Delta I}{L_{eq}} \\ -2k_1\Delta I \\ 0 \end{bmatrix}$
$0 < \Delta v_{ref2} < V_{sat2}$	$A_{312} = \begin{bmatrix} \frac{-R_{eq}}{L_{eq}} & \frac{2}{L_{eq}} & \frac{-2}{L_{eq}} \\ 0 & 0 & 0 \\ 0 & 0 & 0 \end{bmatrix}$, $B_{312} = \begin{bmatrix} \frac{2V_{basediff} - R_{eq}\Delta I}{L_{eq}} \\ 0 \\ -k_1\Delta I \end{bmatrix}$	$A_{322} = \begin{bmatrix} \frac{-R_{eq}}{L_{eq}} & \frac{2}{L_{eq}} & \frac{-2}{L_{eq}} \\ -k_1 & 0 & 0 \\ 0 & 0 & 0 \end{bmatrix}$, $B_{322} = \begin{bmatrix} \frac{2V_{basediff} - R_{eq}\Delta I}{L_{eq}} \\ -2k_1\Delta I \\ -k_1\Delta I \end{bmatrix}$	$A_{332} = \begin{bmatrix} \frac{-R_{eq}}{L_{eq}} & \frac{2}{L_{eq}} & \frac{-2}{L_{eq}} \\ -k_1 & 0 & 0 \\ 0 & 0 & 0 \end{bmatrix}$, $B_{332} = \begin{bmatrix} \frac{2V_{basediff} - R_{eq}\Delta I}{L_{eq}} \\ -2k_1\Delta I \\ -k_1\Delta I \end{bmatrix}$
$\Delta v_{ref2} \ge V_{sat2}$	$A_{313} = \begin{bmatrix} \frac{-R_{eq}}{L_{eq}} & \frac{2}{L_{eq}} & \frac{-2}{L_{eq}} \\ 0 & 0 & 0 \\ 0 & 0 & 0 \end{bmatrix}$, $B_{313} = \begin{bmatrix} \frac{2V_{basediff} - R_{eq}\Delta I}{L_{eq}} \\ 0 \\ -k_1\Delta I \end{bmatrix}$	$A_{323} = \begin{bmatrix} \frac{-R_{eq}}{L_{eq}} & \frac{2}{L_{eq}} & \frac{-2}{L_{eq}} \\ -k_1 & 0 & 0 \\ 0 & 0 & 0 \end{bmatrix}$, $B_{323} = \begin{bmatrix} \frac{2V_{basediff} - R_{eq}\Delta I}{L_{eq}} \\ -2k_1\Delta I \\ -k_1\Delta I \end{bmatrix}$	$A_{333} = \begin{bmatrix} \frac{-R_{eq}}{L_{eq}} & \frac{2}{L_{eq}} & \frac{-2}{L_{eq}} \\ -k_1 & 0 & 0 \\ 0 & 0 & 0 \end{bmatrix}$, $B_{333} = \begin{bmatrix} \frac{2V_{basediff} - R_{eq}\Delta I}{L_{eq}} \\ -2k_1\Delta I \\ -k_1\Delta I \end{bmatrix}$

Table C.6: $C_{\alpha\beta\gamma}$ and $D_{\alpha\beta\gamma}$ for Regions where $(-2\Delta I) < i_d < -\Delta I$.

	$\Delta v_{ref1} \le 0$	$0 < \Delta v_{ref1} < V_{sat1}$	$\Delta v_{ref1} \ge V_{sat1}$
$\Delta v_{ref2} \le 0$	$C_{311} = \begin{bmatrix} 1 & 0 & 0 \\ -1 & 0 & 0 \\ 0 & 0 & 0 \\ 0 & -1 & 0 \\ 0 & 0 & 0 \\ 0 & 0 & -1 \end{bmatrix}$, $D_{311} = \begin{bmatrix} 2\Delta I \\ -\Delta I \\ 0 \\ 0 \\ 0 \\ 0 \end{bmatrix}$	$C_{321} = \begin{bmatrix} 1 & 0 & 0 \\ -1 & 0 & 0 \\ 0 & 1 & 0 \\ 0 & -1 & 0 \\ 0 & 0 & 0 \\ 0 & 0 & -1 \end{bmatrix}$, $D_{321} = \begin{bmatrix} 2\Delta I \\ -\Delta I \\ 0 \\ V_{sat1} \\ 0 \\ 0 \end{bmatrix}$	$C_{331} = \begin{bmatrix} 1 & 0 & 0 \\ -1 & 0 & 0 \\ 0 & 1 & 0 \\ 0 & 0 & 0 \\ 0 & 0 & 0 \\ 0 & 0 & -1 \end{bmatrix}$, $D_{331} = \begin{bmatrix} 2\Delta I \\ -\Delta I \\ -V_{sat1} \\ 0 \\ 0 \\ 0 \end{bmatrix}$
$0 < \Delta v_{ref2} < V_{sat2}$	$C_{312} = \begin{bmatrix} 1 & 0 & 0 \\ -1 & 0 & 0 \\ 0 & 0 & 0 \\ 0 & -1 & 0 \\ 0 & 0 & 1 \\ 0 & 0 & -1 \end{bmatrix}$, $D_{312} = \begin{bmatrix} 2\Delta I \\ -\Delta I \\ 0 \\ 0 \\ 0 \\ V_{sat2} \end{bmatrix}$	$C_{322} = \begin{bmatrix} 1 & 0 & 0 \\ -1 & 0 & 0 \\ 0 & 1 & 0 \\ 0 & -1 & 0 \\ 0 & 0 & 1 \\ 0 & 0 & -1 \end{bmatrix}$, $D_{322} = \begin{bmatrix} 2\Delta I \\ -\Delta I \\ 0 \\ V_{sat1} \\ 0 \\ V_{sat2} \end{bmatrix}$	$C_{332} = \begin{bmatrix} 1 & 0 & 0 \\ -1 & 0 & 0 \\ 0 & 1 & 0 \\ 0 & 0 & 0 \\ 0 & 0 & 1 \\ 0 & 0 & -1 \end{bmatrix}$, $D_{332} = \begin{bmatrix} 2\Delta I \\ -\Delta I \\ -V_{sat1} \\ 0 \\ 0 \\ V_{sat2} \end{bmatrix}$
$\Delta v_{ref2} \ge V_{sat2}$	$C_{313} = \begin{bmatrix} 1 & 0 & 0 \\ -1 & 0 & 0 \\ 0 & 0 & 0 \\ 0 & -1 & 0 \\ 0 & 0 & 1 \\ 0 & 0 & 0 \end{bmatrix}$, $D_{313} = \begin{bmatrix} 2\Delta I \\ -\Delta I \\ 0 \\ 0 \\ -V_{sat2} \\ 0 \end{bmatrix}$	$C_{323} = \begin{bmatrix} 1 & 0 & 0 \\ -1 & 0 & 0 \\ 0 & 1 & 0 \\ 0 & -1 & 0 \\ 0 & 0 & 1 \\ 0 & 0 & 0 \end{bmatrix}$, $D_{323} = \begin{bmatrix} 2\Delta I \\ -\Delta I \\ 0 \\ V_{sat1} \\ -V_{sat2} \\ 0 \end{bmatrix}$	$C_{333} = \begin{bmatrix} 1 & 0 & 0 \\ -1 & 0 & 0 \\ 0 & 1 & 0 \\ 0 & 0 & 0 \\ 0 & 0 & 1 \\ 0 & 0 & 0 \end{bmatrix}$, $D_{333} = \begin{bmatrix} 2\Delta I \\ -\Delta I \\ -V_{sat1} \\ 0 \\ -V_{sat2} \\ 0 \end{bmatrix}$

Table C.7: $A_{\alpha\beta\gamma}$ and $B_{\alpha\beta\gamma}$ for Regions where $i_d < -2\Delta I$.

	$\Delta v_{ref1} \le 0$	$0 < \Delta v_{ref1} < V_{sat1}$	$\Delta v_{ref1} \ge V_{sat1}$
$\Delta v_{ref2} \le 0$	$A_{411} = \begin{bmatrix} \frac{-R_{eq}}{L_{eq}} & \frac{2}{L_{eq}} & \frac{-2}{L_{eq}} \\ -k_1 & 0 & 0 \\ 0 & 0 & 0 \end{bmatrix}$, $B_{411} = \begin{bmatrix} \frac{2V_{basediff} - R_{eq}\Delta I}{L_{eq}} \\ -2k_1\Delta I \\ 0 \end{bmatrix}$	$A_{421} = \begin{bmatrix} \frac{-R_{eq}}{L_{eq}} & \frac{2}{L_{eq}} & \frac{-2}{L_{eq}} \\ -k_1 & 0 & 0 \\ 0 & 0 & 0 \end{bmatrix}$, $B_{421} = \begin{bmatrix} \frac{2V_{basediff} - R_{eq}\Delta I}{L_{eq}} \\ -2k_1\Delta I \\ 0 \end{bmatrix}$	$A_{431} = \begin{bmatrix} \frac{-R_{eq}}{L_{eq}} & \frac{2}{L_{eq}} & \frac{-2}{L_{eq}} \\ 0 & 0 & 0 \\ 0 & 0 & 0 \end{bmatrix}$, $B_{431} = \begin{bmatrix} \frac{2V_{basediff} - R_{eq}\Delta I}{L_{eq}} \\ 0 \\ 0 \end{bmatrix}$
$0 < \Delta v_{ref2} < V_{sat2}$	$A_{412} = \begin{bmatrix} \frac{-R_{eq}}{L_{eq}} & \frac{2}{L_{eq}} & \frac{-2}{L_{eq}} \\ -k_1 & 0 & 0 \\ 0 & 0 & 0 \end{bmatrix}$, $B_{412} = \begin{bmatrix} \frac{2V_{basediff} - R_{eq}\Delta I}{L_{eq}} \\ -2k_1\Delta I \\ -k_1\Delta I \end{bmatrix}$	$A_{422} = \begin{bmatrix} \frac{-R_{eq}}{L_{eq}} & \frac{2}{L_{eq}} & \frac{-2}{L_{eq}} \\ -k_1 & 0 & 0 \\ 0 & 0 & 0 \end{bmatrix}$, $B_{422} = \begin{bmatrix} \frac{2V_{basediff} - R_{eq}\Delta I}{L_{eq}} \\ -2k_1\Delta I \\ -k_1\Delta I \end{bmatrix}$	$A_{432} = \begin{bmatrix} \frac{-R_{eq}}{L_{eq}} & \frac{2}{L_{eq}} & \frac{-2}{L_{eq}} \\ 0 & 0 & 0 \\ 0 & 0 & 0 \end{bmatrix}$, $B_{432} = \begin{bmatrix} \frac{2V_{basediff} - R_{eq}\Delta I}{L_{eq}} \\ 0 \\ -k_1\Delta I \end{bmatrix}$
$\Delta v_{ref2} \ge V_{sat2}$	$A_{413} = \begin{bmatrix} \frac{-R_{eq}}{L_{eq}} & \frac{2}{L_{eq}} & \frac{-2}{L_{eq}} \\ -k_1 & 0 & 0 \\ 0 & 0 & 0 \end{bmatrix}$, $B_{413} = \begin{bmatrix} \frac{2V_{basediff} - R_{eq}\Delta I}{L_{eq}} \\ -2k_1\Delta I \\ -k_1\Delta I \end{bmatrix}$	$A_{422} = \begin{bmatrix} \frac{-R_{eq}}{L_{eq}} & \frac{2}{L_{eq}} & \frac{-2}{L_{eq}} \\ -k_1 & 0 & 0 \\ 0 & 0 & 0 \end{bmatrix}$, $B_{422} = \begin{bmatrix} \frac{2V_{basediff} - R_{eq}\Delta I}{L_{eq}} \\ -2k_1\Delta I \\ -k_1\Delta I \end{bmatrix}$	$A_{433} = \begin{bmatrix} \frac{-R_{eq}}{L_{eq}} & \frac{2}{L_{eq}} & \frac{-2}{L_{eq}} \\ 0 & 0 & 0 \\ 0 & 0 & 0 \end{bmatrix}$, $B_{433} = \begin{bmatrix} \frac{2V_{basediff} - R_{eq}\Delta I}{L_{eq}} \\ 0 \\ -k_1\Delta I \end{bmatrix}$

Table C.8: $C_{\alpha\beta\gamma}$ and $D_{\alpha\beta\gamma}$ for Regions where $i_d < -2\Delta I$.

	$\Delta v_{ref1} \le 0$	$0 < \Delta v_{ref1} < V_{sat1}$	$\Delta v_{ref1} \ge V_{sat1}$
$\Delta v_{ref2} \le 0$	$C_{411} = \begin{bmatrix} 0 & 0 & 0 \\ -1 & 0 & 0 \\ 0 & 0 & 0 \\ 0 & -1 & 0 \\ 0 & 0 & 0 \\ 0 & 0 & -1 \end{bmatrix}$, $D_{411} = \begin{bmatrix} 0 \\ -2\Delta I \\ 0 \\ 0 \\ 0 \\ 0 \end{bmatrix}$	$C_{421} = \begin{bmatrix} 0 & 0 & 0 \\ -1 & 0 & 0 \\ 0 & 1 & 0 \\ 0 & -1 & 0 \\ 0 & 0 & 0 \\ 0 & 0 & -1 \end{bmatrix}$, $D_{421} = \begin{bmatrix} 0 \\ -2\Delta I \\ 0 \\ V_{sat1} \\ 0 \\ 0 \end{bmatrix}$	$C_{431} = \begin{bmatrix} 0 & 0 & 0 \\ -1 & 0 & 0 \\ 0 & 1 & 0 \\ 0 & 0 & 0 \\ 0 & 0 & 0 \\ 0 & 0 & -1 \end{bmatrix}$, $D_{431} = \begin{bmatrix} 0 \\ -2\Delta I \\ -V_{sat1} \\ 0 \\ 0 \\ 0 \end{bmatrix}$
$0 < \Delta v_{ref2} < V_{sat2}$	$C_{412} = \begin{bmatrix} 0 & 0 & 0 \\ -1 & 0 & 0 \\ 0 & 0 & 0 \\ 0 & -1 & 0 \\ 0 & 0 & 1 \\ 0 & 0 & -1 \end{bmatrix}$, $D_{412} = \begin{bmatrix} 0 \\ -2\Delta I \\ 0 \\ 0 \\ 0 \\ V_{sat2} \end{bmatrix}$	$C_{422} = \begin{bmatrix} 0 & 0 & 0 \\ -1 & 0 & 0 \\ 0 & 1 & 0 \\ 0 & -1 & 0 \\ 0 & 0 & 1 \\ 0 & 0 & -1 \end{bmatrix}$, $D_{422} = \begin{bmatrix} 0 \\ -2\Delta I \\ 0 \\ V_{sat1} \\ 0 \\ V_{sat2} \end{bmatrix}$	$C_{432} = \begin{bmatrix} 0 & 0 & 0 \\ -1 & 0 & 0 \\ 0 & 1 & 0 \\ 0 & 0 & 0 \\ 0 & 0 & 1 \\ 0 & 0 & -1 \end{bmatrix}$, $D_{432} = \begin{bmatrix} 0 \\ -2\Delta I \\ -V_{sat1} \\ 0 \\ 0 \\ V_{sat2} \end{bmatrix}$
$\Delta v_{ref2} \ge V_{sat2}$	$C_{413} = \begin{bmatrix} 0 & 0 & 0 \\ -1 & 0 & 0 \\ 0 & 0 & 0 \\ 0 & -1 & 0 \\ 0 & 0 & 1 \\ 0 & 0 & 0 \end{bmatrix}$, $D_{413} = \begin{bmatrix} 0 \\ -2\Delta I \\ 0 \\ 0 \\ -V_{sat2} \\ 0 \end{bmatrix}$	$C_{423} = \begin{bmatrix} 0 & 0 & 0 \\ -1 & 0 & 0 \\ 0 & 1 & 0 \\ 0 & -1 & 0 \\ 0 & 0 & 1 \\ 0 & 0 & 0 \end{bmatrix}$, $D_{423} = \begin{bmatrix} 0 \\ -2\Delta I \\ 0 \\ V_{sat1} \\ -V_{sat2} \\ 0 \end{bmatrix}$	$C_{433} = \begin{bmatrix} 0 & 0 & 0 \\ -1 & 0 & 0 \\ 0 & 1 & 0 \\ 0 & 0 & 0 \\ 0 & 0 & 1 \\ 0 & 0 & 0 \end{bmatrix}$, $D_{433} = \begin{bmatrix} 0 \\ -2\Delta I \\ -V_{sat1} \\ 0 \\ -V_{sat2} \\ 0 \end{bmatrix}$

Bibliography

[1] J. Lunze, *Feedback Control of Large-Scale Systems*. New York: Prentice-Hall, Chapter 12, 1992.

[2] M. Johansson and A. Rantzer, "Computation of Piecewise Quadratic Lyapunov Functions for Hybrid Systems," Department of Automatic Control, Lund Institute of Technology, June 1997.

[3] M. Johansson and A. Rantzer, *Piecewise Linear Control Toolbox*, Department of Automatic Control, Lund Institute of Technology, June 1997.

[4] The Mathworks, Inc., Natick, MA. *LMI Control Toolbox For Use with Matlab*, 1995.

[5] M. Vidyasagar, *Nonlinear Systems Analysis*. New Jersey: Prentice-Hall, 1993.

[6] M. Jordan, "*UC3907* Load Share IC Simplifies Parallel Power Supply Design," *Unitrode Application Note U-129*, Unitrode Corp., Merrimack, NH, 1990.

[7] D. J. Perreault, J. G. Kassakian, and G. C. Verghese, "Stability Analysis of Nonlinear Current-Sharing Techniques," *1997 IEEE Power Electronics Specialists Conference*, pp. 665-671, June 1997.

[8] D. J. Perreault, R. Selders, and J. G. Kassakian, "Frequency-Based Current-Sharing Techniques for Paralleled Power Converters", *1996 IEEE Power Electronics Specialists Conference*, Baveno, Italy, pp. 1073-1080, June 1996.

[9] D. J. Perreault, R. L. Selders, and J. G. Kassakian, "Implementation and Evaluation of a Frequency-Based Current-Sharing Technique for Cellular Converter Systems", *IEEE Africon '96*, Matieland, South Africa, pp. 682-686, Sept. 1996.

[10] D. Maliniak, "Dense DC-DC Converters Actively Share Stress," *Electronic Design*, pp. 39-44, Jan. 1993.

[11] R. L. Selders, "A Current-Balancing Control System for Cellular Power Converters", S.M. Thesis, *M.I.T. Department of Electrical Engineering and Computer Science*, Feb. 1996.

[12] V. J. Thottuvelil and G. C. Verghese, "Analysis and Control Design of Paralleled DC/DC Converters with Current Sharing," *1997 IEEE Applied Power Electronics Conference*, pp. 638-646, Feb. 1997.

[13] T. Kohama, T. Ninomiya, M. Shoyama, and F. Ihara, "Dynamic Analysis of Parallel Module Converter System with Current Balance Controllers," *1994 IEEE Telecommunications Energy Conference Record*, pp. 190-195, 1994.

[14] D. S. Garabandic and T. B. Petrovic, "Modeling Parallel Operating PWM DC/DC Power Supplies," *IEEE Trans. Industrial Electronics*, Vol. 42, No. 5, pp. 545-551, Oct. 1995.

[15] Y. Panov, J. Rajagopalan, and F. C. Lee, "Analysis and Design of *N* Paralleled DC-DC Converters with Master-Slave Current-Sharing Control," *1997 IEEE Applied Power Electronics Conference*, pp. 436-442, Feb. 1997.